Zoological Journal of the Linnean Society, 2020, **190**, 271–297. With 11 figures.

Lizards from the Lost World: two new species and evolutionary relationships of the Pantepui highland *Riolama* (Gymnophthalmidae)

RENATO RECODER[1*], IVAN PRATES[2], SERGIO MARQUES-SOUZA[1], AGUSTÍN CAMACHO[1], PEDRO M. SALES NUNES[3], FRANCISCO DAL VECHIO[1], JOSÉ MARIO GHELLERE[1], ROY W. MCDIARMID[2] and MIGUEL TREFAUT RODRIGUES[1]

[1]*Departamento de Zoologia, Instituto de Biociências, Universidade de São Paulo, São Paulo, Brazil*
[2]*Department of Vertebrate Zoology, National Museum of Natural History, Smithsonian Institution, Washington, DC, USA*
[3]*Departamento de Zoologia, Centro de Biociências, Universidade Federal de Pernambuco, Recife, Pernambuco, Brazil*

Received 7 July 2019; revised 21 November 2019; accepted for publication 1 December 2019

The Pantepui region of northern South America harbours an endemic fauna that differs dramatically from those of the surrounding lowland rainforests and savannas. A component of this unique fauna is *Riolama*, a poorly known genus of microteiid lizards with four described and two undescribed species restricted to tepui mountains. We here implement an integrative approach to formally describe the two unnamed species and investigate the phylogenetic relationships and timing of diversification in *Riolama* using a fossil-calibrated molecular approach. Our results suggest that diversification initiated in *Riolama* during the Oligocene (*c.* 28 Mya), thereby characterizing the genus as an ancient lineage. This supports the Plateau biogeographic hypothesis to explain the diversification of the Pantepui fauna. Our divergence time estimation analysis also provides an updated temporal framework for the diversification of the highly diverse Gymnophthalmidae clade.

ADDITIONAL KEYWORDS: diversity – endemism – herpetofauna – MRCA – taxonomy – tepui.

INTRODUCTION

Tepuis are the table mountains in northern South America that inspired Sir Arthur Conan Doyle's dreams of a lost world inhabited by an ancient fauna (Doyle, 1912). These rise sharply from the surrounding landscape, with the summits reaching between 1200 and 2995 m a.s.l. across the Roraima formation of the Guiana Shield, composing the discontinuous biogeographic province of Pantepui (Huber, 1987; Rull, 2004). The numerous sandstone table-top mountains of the Pantepui date back to the Precambrian at around 2 billion years ago, ranking this region among the oldest surface rocks on Earth (Huber, 1995; McDiarmid & Donnelly, 2005). Isolated tepui mountains function as 'sky islands' that harbour ecological communities different to those of the surrounding lowland rainforests and savannas (McDiarmid *et al.*, 1988; McDiarmid & Donnelly, 2005; Kok *et al.*, 2012).

Biogeographic hypotheses have been proposed to explain the origin and diversification of the Pantepui endemic fauna (Mayr & Phelps, 1967), with three being the most debated for low-vagile groups such as amphibians and reptiles (Hoogmoed, 1979; McDiarmid & Donnelly, 2005): the 'Plateau Hypothesis', which proposes that erosion of a previously continuous tableland promoted vicariant diversification of widespread ancestral summit species; the 'Cool Climate Hypothesis', which postulates that cooler Quaternary climates allowed dispersal of summit species across tepuis through the lowlands; and the 'Habitat Shift Hypothesis', which hypothesizes that cycles of upland colonization of tepui summits from lowland ancestral species occurred owing to shifts in habitat preference.

*Corresponding author. E-mail: renatorecoder@gmail.com
[Version of record, published online 27 January 2020; http://zoobank.org/ urn:lsid:zoobank.org:pub:1658E4C8-C054-46B1-8508-F79D945D371D]

© 2020 The Linnean Society of London,

Downloaded from https://academic.oup.com/zoolinnean/article/190/1/271/5716277 by guest on 25 April 2024

Molecular studies of the endemic upland Pantepui herpetofauna provided variable support for each of these hypotheses. Some suggested that diversification in several groups is more recent than previously thought, given the old geological history of the tepui highlands, thus supporting a predominant role of dispersal between summits (Kok *et al.*, 2012; Salerno *et al.*, 2012). Nevertheless, some upland Pantepui frogs exhibit split ages much older than the Pleistocene, despite close relationships between highland species, supporting a possible role of vicariance for diversification on the tepuis (Kok *et al.*, 2016, 2017).

Amphibians and reptiles represent a remarkable component of the Pantepui, with up to 80% of the highland species considered to be endemic (Hoogmoed, 1979; McDiarmid & Donnelly, 2005). Despite multinational efforts to perform herpetological inventories in various tepui over the last three decades, most species remain undescribed (McDiarmid *et al.*, 1988; McDiarmid & Donnelly, 2005).

Among the clades that are restricted to the Pantepui highlands is the lizard genus *Riolama* Uzzell, 1973, one of the poorest known groups of Gymnophthalmidae (Pellegrino *et al.*, 2001; Goicoechea *et al.*, 2016). Four species have been formally described: *Riolama inopinata* Kok, 2015, *R. leucosticta* (Boulenger, 1900), *R. luridiventris* Esqueda, La Marca & Praderio, 2004 and *R. uzzelli* Molina & Señaris, 2003; all from sites above 1800 m. Most species are known from few specimens, few localities and are thus rare in zoological collections (Esqueda *et al.*, 2004; McDiarmid & Donnelly, 2005). *Riolama* was not represented in phylogenetic analyses, until molecular data from *R. inopinata* and *R. leucosticta* provided support for the recognition of Riolaminae, a new subfamily in Gymnophthalmidae (Kok, 2015). Given the highly disjunct distribution of *Riolama* species among isolated tepui, an improved knowledge of the phylogenetic relationships within the genus, and the timing of its diversification with respect to other Gymnophthalmidae, can help us to understand the origins and evolutionary relationships of the Pantepui biota.

In the 1980s, an American–Venezuelan joint programme of field expeditions sampled two new species of *Riolama* on the Cerro Neblina highlands in southern Venezuela (McDiarmid *et al.*, 1988). During an expedition supported by the Brazilian army, with the participation of local Yanomami communities, we surveyed the highest part of the Brazilian portion of this tepui complex, situated in the Pico da Neblina National Park. There, we obtained specimens and tissue samples from the two additional, yet undescribed *Riolama*. We here implement an integrative approach to investigate the phylogenetic relationships and the timing of diversification of *Riolama* using a fossil-calibrated molecular approach, and formally describe these two new species. Our results add elements to our understanding of the origins and diversification of the Pantepui biota and provide a temporal framework for the diversification of the highly diverse Gymnophthalmidae clade. We also include data on the natural history and thermal physiology of these rare species, shedding light on factors that may restrict them to higher elevations.

MATERIAL AND METHODS

Habitat and ecology

Serra da Neblina is one of the most unexplored highland areas in South America outside of the Andes (Steyermark *et al.*, 1995). This large sandstone massif covers an area about 50 km long and 20 km wide along a north-eastern to south-western direction near the Venezuela–Brazil border. Most of its area lies in Venezuelan, but with 2995 m, the Pico da Neblina is the highest point and the highest mountain in Brazil. The region is still pristine and mostly falls within Parque Nacional do Pico da Neblina in Brazil and Parque Nacional de la Serrania de Neblina in Venezuela, both broadly overlapping with the Yanomami territory. The massif emerges from the lowlands covered by Amazonian forest that extends up to about 1000 m. Above 1000 m, the area is irregularly covered with high and low montane forests until up to about 1800 m, above which montane forests give way to open landscapes dominated by low scrub with scattered trees and large fields of bromeliads and meadows on peat that become bogs after rain, at the plateaus and highest peaks. According to Steyermark (1986), the Neblina massif houses the highest plant diversity of the Pantepui, and it may have the highest level of plant endemism in the Guiana Shield.

The Brazilian expedition concentrated its exploration around the region of Bacia do Gelo, an extensive plateau of around 2000 m elevation facing the Pico da Neblina (Figs 1, 2A, D–F). The plateau and some scattered isolated mountains bordering it are drained by a mid-sized stream (*c.* 2-m wide) with clear water that overflows after heavy rains and floods the plateau (Fig. 2A, D). Local vegetation is dominated by small to mid-sized shrubs and meadows where Bromeliaceae (especially *Brocchinia tatei* L.B.Sm.), Rapateaceae and Theaceae are abundant in the mostly wet peat (Fig. 2A, B, E). However, some areas, especially those near the slopes of the isolated mountains, are covered by a denser and taller vegetation (up to 5 m) where palms (*Euterpe* sp.) are frequent (Fig. 2D, F). In both habitats, the soil is dominated by peat with scattered patches of sand and rocks.

Downloaded from https://academic.oup.com/zoolinnean/article/190/1/271/5716277 by guest on 25 April 2024

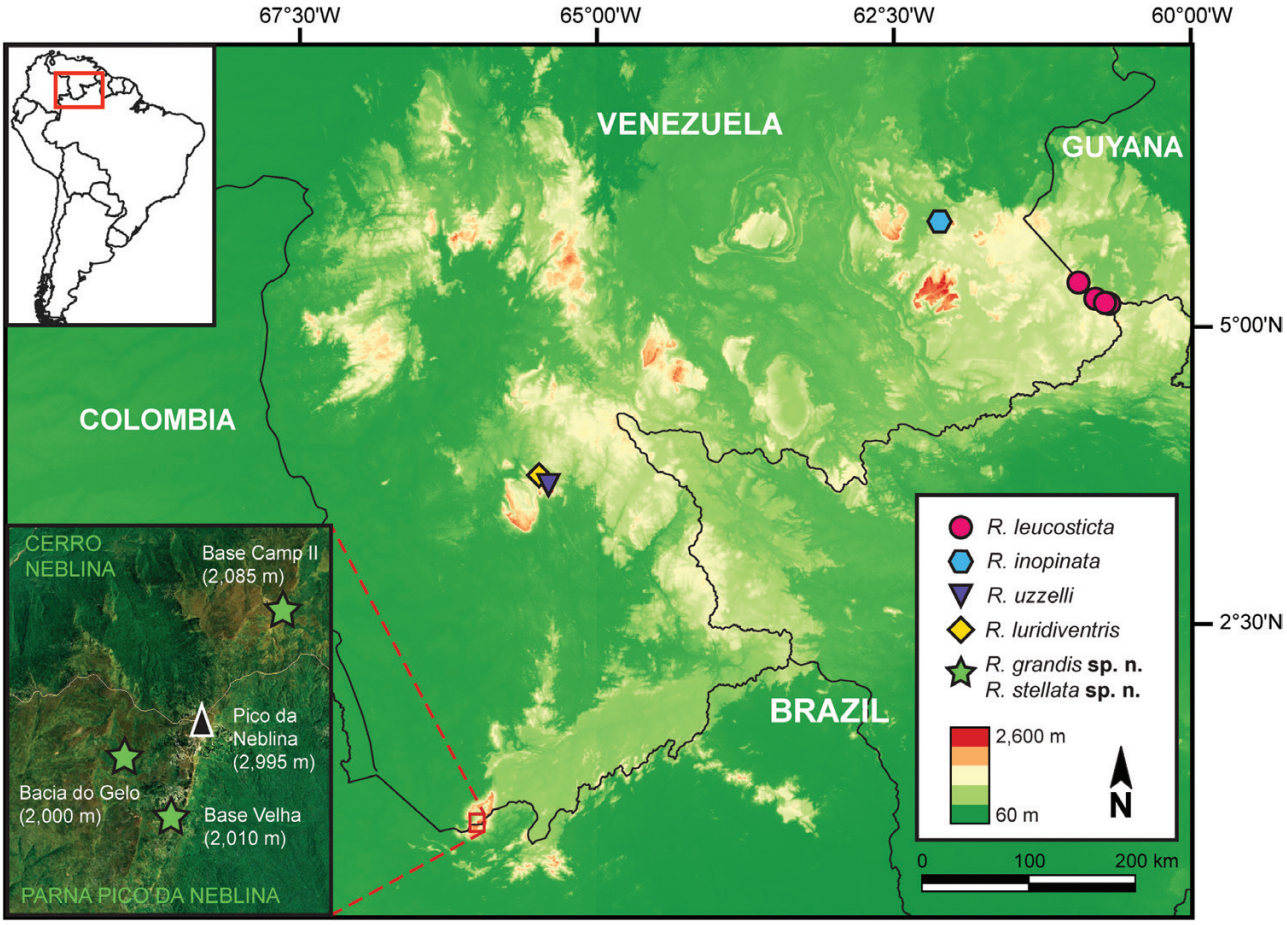

Figure 1. Map of Pantepui region in northern South America, showing the distribution of *Riolama* species. The inset shows the sampling localities (green stars) where *Riolama grandis* and *Riolama stellata* were collected at the Neblina highlands, all above 2000 m of elevation. Aerial image from Google Earth Pro 2019 DigitalGlobe Image Landsat/Copernicus.

The American–Venezuelan fieldwork focused around Camp II, an area encompassing three different sites located between 2085 and 2100 m in a shallow valley lying 2.5 to 3.5 km north-east of Pico da Neblina in the southern portion of the massif (McDiarmid & Donelly, 2005). A small stream flows north through the valley into the Cañon Grande. The valley contains a mosaic of habitats: bogs occur in the poorly drained areas and are dominated by pitcher plants (*Heliamphora neblinae* Maguire, Sarraceniaceae), *Tillandsia* sp. (Bromeliaceae), sedges and similar plants. Dense stands of bromeliads (*Brocchinia tatei*) occur on the better drained sites. The stream is bordered by a low-stature gallery forest that includes palms (*Euterpe* sp.) and other small trees. The slopes are steep, often rocky and vegetated by stands of *Bonnetia* sp. (Bonnetiaceae). The actual camp sites were located in the more open, boggy areas. Both lizard species were found in tents in these boggy areas.

Specimens of *Riolama* sp. nov. a *sensu* McDiarmid *et al.* (1988) were collected in Bacia do Gelo through pitfall traps installed in open habitats (N = 2) and by hand in Bacia do Gelo and Base Velha camp (N = 8). Some specimens were collected in grassy meadows and were active on sunny days. Two specimens were obtained when crossing horizontal fallen trunks 0.4 m above soil between clusters of vegetation. Both Venezuelan specimens of *Riolama* sp. nov. a *sensu* McDiarmid *et al.* (1988) were collected about a year apart in Camp II. One individual (AMNH-R-178714, R.G. Zweifel unpublished field notes) was found extremely active under a small pack inside a tent.

The four Brazilian specimens of *Riolama* sp. nov. b *sensu* McDiarmid *et al.* (1988) were captured in areas with dense vegetation. Two were collected in pitfall traps, one after a heavy rain, in a peat bog covered by trees reaching 4–5 m high. The other two were found active on the ground near the base camp. The Venezuelan specimens of *Riolama* sp. nov. b *sensu* McDiarmid *et al.* (1988) were collected in all three sites around Camp II during the day. A few were active during brief sunny periods and moved through and over clumps of grass-like vegetation around the camp.

Downloaded from https://academic.oup.com/zoolinnean/article/190/1/271/5716277 by guest on 25 April 2024

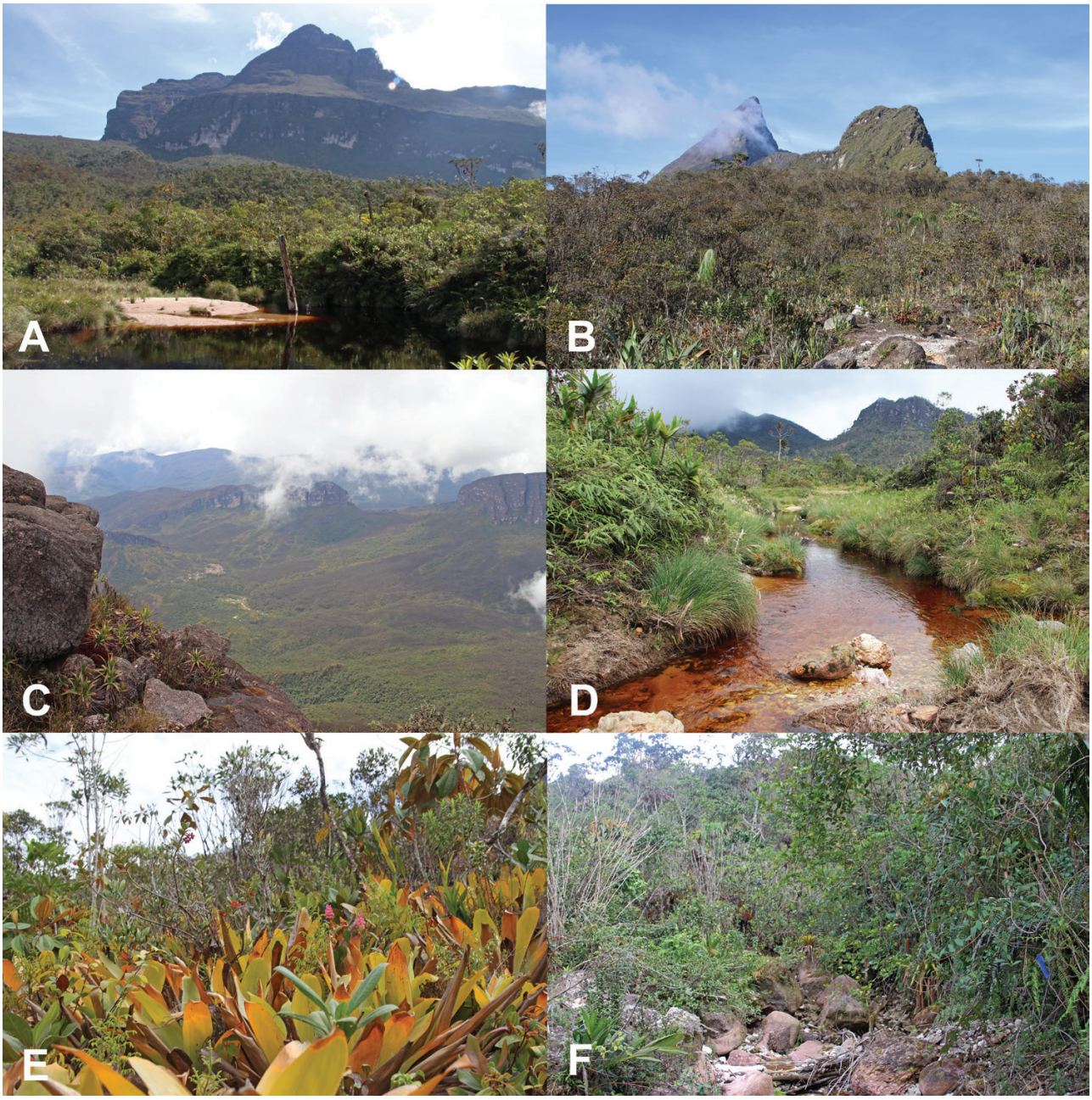

Figure 2. Habitat and landscape: A, view of Pico da Neblina summit from Bacia do Gelo basecamp; B, view of Pico da Neblina summit from Base Velha basecamp; C, panoramic view of Neblina plateau from Pico da Neblina massif, close to the summit –Bacia do Gelo basecamp area can be observed in the centre-left; D, stream and marginal vegetation at Bacia do Gelo; E, open habitat with clusters of Bromeliaceae; F, dense semi-arboreal vegetation in steep terrain.

Most were found 'swimming' in the mixture of plants, moss, water and mud (0.3–0.5 m deep) that resulted from the activities of the scientists moving around the camp and the frequent and heavy rain. Both species are currently known only from the highlands of Serra da Neblina (Cerro Neblina) at elevations above 2000 m a.s.l (Fig. 1), where they are found in syntopy.

SAMPLING OF SPECIMENS

Specimens of *Riolama* spp. were collected by hand or in pitfall traps, killed by injection of 5% lidocaine solution, fixed in 10% formalin and preserved in 70% ethanol. Pitfall traps consisted of 25 sampling units of four buckets buried at ground level and connected by plastic fences, which remained open between 16 and 22 November

Downloaded from https://academic.oup.com/zoolinnean/article/190/1/271/5716277 by guest on 25 April 2024

2017, totalling an effort of 700 buckets. Prior to fixation, we obtained tissue samples (a piece of liver or muscle preserved in 95% ethanol) from some individuals for molecular analysis. Voucher specimens were deposited in the collections of the Smithsonian National Museum of Natural History (USNM), American Museum of Natural History (AMNH) and Museu de Zoologia da Universidade de São Paulo (MZUSP).

Morphological data and analysis

We examined external morphological characters of preserved specimens under a stereomicroscope. We took 12 morphometric measurements with a digital calliper to the nearest 0.01 mm (rounded to nearest 0.1 mm), as follows: snout–vent length, from the tip of snout to the posterior margin of the cloaca (SVL); trunk-length, from the anterior margin of the forelimbs to the posterior margins of the hindlimbs (TRL); head height at the highest point in a longitudinal axis (HH); head width at the widest point (HW); head length, from the tip of the snout to the anterior margin of the ear opening (HL); eye–snout distance, from the tip of the snout to the anterior margin of the eye (ESD); femur length, from the lateral margin of the cloacal plate to the knee joint (FEM); tibia length, from the knee joint to the margin of the sole (TIB); foot length, from the proximal margin of the sole to the tip of the fourth toe, excluding the claw (FTL); humeral length, from the axilla to the elbow joint (HUM); hand length, from the elbow joint to the tip of the fourth finger, excluding the claw (HAL); and tail length, from the posterior margin of the cloacal aperture to the tip of the tail (TAL) in individuals with unbroken tails. Additionally, we measured extended forelimb length (FLL) and extended hindlimb length (HLL) to compare limb proportions among species.

We took ten scale count traits: number of transversal rows of dorsal scales, between the postoccipitals and the posterior insertion of the hindlimbs in a mid-dorsal line (DOR); number of transversal rows of ventral scales at the mid-body (VEN); number of transverse rows of gular scales between the postmental groove and the collar fold (GUL); number of longitudinal rows of scales around the mid-body (SAM); number of subdigital lamellae under the fourth finger (4FL); number of subdigital lamellae under the fourth toe (4TL); number of supralabial scales (SL); number of infralabial scales (IL); total number of femoral pores (POR); and number of scales around the tail at the third row of scales (SAT). Statistical differences in body size (SVL) between sexes were tested using analysis of variance (ANOVA), while differences in proportions (based on the remaining morphometric characters) were tested using analysis of covariance (ANCOVA) with SVL as a covariate. Statistical analyses were performed using R (R Core Team, 2019).

We performed comparisons of external morphology among the new species and the four currently known species of *Riolama* based on original descriptions (Boulenger, 1900; Molina & Señaris, 2003; Esqueda *et al.*, 2004; Kok, 2015).

Hemipenis

The hemipenes of one paratype of both the new species and one specimen of *R. leucosticta* were prepared following the procedures described by Manzani & Abe (1988), modified by Pesantes (1994) and Zaher (1999). The retractor muscle was manually separated, and the everted organ was filled with stained petroleum jelly. The organs were immersed in an alcoholic solution of Alizarin Red for 24 hours in order to stain calcified structures (e.g. spines or spicules), a modification proposed by Nunes *et al.* (2012) on the procedures described by Uzzell (1973) and Harvey & Embert (2008). The terminology of hemipenial structures follows previous literature (Dowling & Savage, 1960; Savage, 1997; Myers *et al.*, 2009; Nunes *et al.*, 2012).

Generation of molecular data

We extracted genomic DNA from tissue samples following the protocol described in Fetzner (1999). We obtained sequence fragments of the ribosomal mitochondrial 12S rDNA gene (12S) and 16S rDNA gene (16S), the protein-coding mitochondrial genes cytochrome b (*Cytb*) and NADH dehydrogenase subunit 4 (*ND4*) and the nuclear exons oocyte maturation factor gene (*c-mos*) and neurotrofin-3 gene (*ntf3*). Conditions for polymerase chain reaction amplification, primers and primer sources are given in Table 1. Purification of PCR products was performed with Exonuclease I and Shrimp Alkaline Phosphatase (Thermo Fisher Scientific Inc.). Both strands of each fragment were sequenced using the BigDye Terminator 3.0 Cycle Sequencing Kit (Applied Biosystems) according to the protocol of the manufacturer. PCR products were sequenced at the Instituto de Biociências da Universidade de São Paulo (São Paulo, Brazil). Sequences were edited with GENEIOUS PRO 10 (Kearse *et al.*, 2012). New sequences generated in this study were deposited in the GenBank under accession numbers (MN528013–MN528020; MN555467–MN555482).

For phylogenetic and divergence time estimation, the molecular database was complemented with sequences retrieved from the GenBank (Supporting Information, Table S1) for other *Riolama* species (Kok, 2015) and representatives of Lacertoidea (Gymnophthalmidae, Alopoglossidae, Teiidae, Amphisbaenia, Lacertidae), as

Downloaded from https://academic.oup.com/zoolinnean/article/190/1/271/5716277 by guest on 25 April 2024

Table 1. Molecular markers used in this study. Information about marker type, primers, annealing temperatures and respective references are presented

Gene	Type	Primer: Sequence (5' ➔ 3')	T°C	Reference
12S	mtDNA (ribossomal)	12Sa: CTGGGATTAGATACCCCACTA 12Sb: TGAGGAGGGTGACGGGCGGT	56	Harris *et al.*, 1998
16S	mtDNA (ribossomal)	16S-F: CTGTTTACCAAAAACATMRCCTYTAGC 16S-R: TAGATAGAAACCGACCTGGATT	51	Pellegrino *et al.*, 2001
Cytb	mtDNA (coding)	CB1: CCATCCAACATCTCAGCATGATGAAA CB3: GGCAAATAGGARRTATCATTC	51	Palumbi, 1996
ND4	mtDNA (coding)	ND4-F: CACCTATGACTACCAAAAGCTCATGT AGAAG ND4-R (LEU): CATTACTTTTACTTGGATTTGCACCA	52	Arévalo *et al.*, 1994
c-mos	nuDNA (exon)	G73: GCGGTAAAGCAGGTGAAGAAA G74: TGAGCATCCAAAGTCTCCAATC	53	Saint *et al.*, 1998
ntf3	nuDNA (exon)	NTF3-F1: ATGTCCATCTTGTTTTATGTGATATTT NTF3-R1: ACRAGTTTRTTGTTYTCTGAAGTC	53	Townsend *et al.*, 2008

well as *Iguana iguana* (Linnaeus, 1758) and *Varanus salvator* (Laurenti, 1768) as outgroups (totalling 121 taxa). Alignments were generated using MAFFT 7.309 (Katoh & Standley, 2013) as implemented in GENEIOUS PRO 10 (Kearse *et al.*, 2012) under default settings. We excluded nucleotide sites that show ambiguous homology in the alignments of ribosomal genes using GBlocks 0.91b (Castresana, 2000). Recombination within all loci was rejected based on the *Dss* statistic (McGuire & Wright, 2000) estimated in TOPALi 2.5 (Milne *et al.*, 2009).

Phylogenetic analyses

A concatenated matrix with the six loci combined (12S + 16S + *Cytb* + *ND4* + *c-mos* + *ntf3*; 3418 bp) was generated using SequenceMatrix 1.7 (Vaidya *et al.*, 2011). We selected models of nucleotide substitution using PartitionFinder 2.1.1 (Lanfear *et al.*, 2016), implementing PhyML for likelihood estimation (Guindon *et al.*, 2010) and the Bayesian information criterion for model selection (Sullivan & Joyce, 2005). Based on PartitionFinder results, codon partitions were implemented for the protein-coding genes *Cytb*, *ND4*, *c-mos* and *ntf3* (i.e. three partitions per gene).

We conducted phylogenetic analysis using Bayesian inference (BI) in MrBayes 3.2 (Ronquist *et al.*, 2012) with a reduced dataset focusing on Gymnophthalmidae, Alopoglossidae and Teiidae (the Gymnophthalmoidea clade; 74 sampled taxa). We implemented two independent runs of 50×10^6 generations each, sampled at intervals of 5000 generations; each run included four independent chains. We used TRACER 1.7 (Rambaut *et al.*, 2018) to assess whether Markov chain mixing was adequate (effective sample sizes > 200) and to visually assess model parameter stationarity and convergence between runs. We discarded trees prior to the stationary phase as 'burn-in' (20%) and generated a 50% majority rule consensus tree from the remaining data. Net between-group uncorrected genetic distances among specimens of *Riolama* were calculated in MEGA 7 (Kumar *et al.*, 2016) based on the 16S and *ND4* alignments.

Divergence time estimation

In the absence of fossils nested within Gymnophthalmidae lizards, we performed simultaneous phylogenetic inference and divergence time estimation for the Lacertoidea clade (*sensu* Zheng & Wiens, 2016) incorporating three calibration points (see below). Dating analyses were performed under a Bayesian framework using BEAST 1.10.2 (Suchard *et al.*, 2018) with a birth–death process tree prior (Gernhard, 2008) and an uncorrelated lognormal relaxed clock (Drummond *et al.*, 2006) for each gene separately. We implemented best-fit models of substitution for each gene or codon partition based on the best scheme resulted from PartitionFinder analysis. Three independent BEAST runs of 100 million generations each were performed, sampling every 10 000 generations. We used TRACER to assess proper Markov chain mixing, model parameter stationarity and convergence between runs, as described above for MrBayes analyses. We then combined the three runs in LogCombiner 1.10 (with 20% of each run discarded as burn-in) and summarized a maximum clade credibility tree in TreeAnnotator 1.10 (http://beast.community/treeannotator). The resulting topologies were visualized in FigTree 1.4 (available from http://tree.bio.ed.ac.uk/software/figtree).

We used three calibration points based on two well-known Lacertoidea fossils and one secondary calibration: (1) the most ancient split in crown

Downloaded from https://academic.oup.com/zoolinnean/article/190/1/271/5716277 by guest on 25 April 2024

Amphisbaenia (*Rhineura floridiana* Baird, 1859 vs. Amphisbaeniformes), dated back to the Early Cretaceous (130 Mya) based on a fossil-calibrated analysis (Longrich *et al.*, 2015); (2) the first known Lacertidae, *Cryptolacerta hassiaca* Müller *et al.*, 2011 from the Middle Eocene (41.2–47.8 Mya), first described as an Amphisbaenidae (Müller *et al.*, 2011), but posteriorly recovered as a stem Lacertidae (Longrich *et al.*, 2015); and (3) the oldest known Tupinambinae (including Callopistinae), *Lumbrerasaurus scagliai* Donadio, 1985 from the Early Eocene (58.0–55.5 Mya), considered as *nomen dubium* by Sullivan & Estes (1997) and redescribed as a Tupinambinae by Brizuela & Albino (2016). Prior distributions for each calibrated node were set as follows: for (1) a normal prior with mean 130 Mya and standard deviation of 10 Myr; for (2) a lognormal prior with mean 2.0, standard deviation 0.8 and offset 41 Myr; and for (3) a lognormal prior with mean 2.0, standard deviation 0.8 and offset 55.0 Myr.

Measurement of thermal tolerance

To better characterize the ecological tolerances of highland tepui lizards, we measured the voluntary thermal maximum (VTM) of two specimens of *Riolama* sp. nov. a *sensu* McDiarmid *et al.* (1988). This parameter describes the maximum temperature a lizard withstands before leaving a warmed refuge, and exposure to such temperature threshold is often fatal within three hours (Camacho *et al.*, 2018). The VTM was measured following the 'dark chamber protocol' described in detail by Camacho *et al.* (2018). In short, each lizard was progressively heated within a metal can until it left it. Specimens had their body temperatures measured twice: at the start of the heating process and right after leaving the can. Temperatures were measured using a thermal camera (FLIR C2), with distance parameter set to 0.20 m, the emissivity to 0.80 and the measuring pointer aiming to the dorsum of the animal. A heating tape wrapped externally to the can heated the interior homogeneously with a starting temperature of 24 °C and heating rate of 1.3 °C/min. An opaque plastic lid could be opened by the lizard from the inside, allowing the animal to exit the interior at any moment. Specimens were kept in plastic bags covered with vegetation for less than 24 hours before the experiments.

The VTM can be combined with an estimation of the minimum temperature available in a given habitat (usually air temperature measured in the shade; e.g. Huey *et al.*, 2009) to identify when environmental temperatures become stressful (i.e. too hot) for a species (Camacho *et al.*, 2018). To approximate the minimum temperatures across the known distribution of the new species, we obtained air temperatures from ~1 km resolution bioclimatic raster layer from the WorldClim 2 dataset (Fick & Hijmans, 2017). By subtracting the maximum air temperature in the shade to the voluntary thermal maximum, we obtained a map of 'thermal safety margins', where negative values indicate regions expected to represent physiologically stressful air temperatures for this species.

RESULTS

Hemipenial morphology

The hemipenial morphology of *Riolama* sp. nov. a and *R.* sp. nov. b *sensu* McDiarmid *et al.* (1988) (this study: Fig. 3A, B), *R. leucosticta* (Boulenger, 1900) (Nunes, 2011; Fig. 3C) and *R. inopinata* Kok, 2015 is overall similar regarding the position and type of the ornamentation on hemipenial bodies, although some specific differences are noticed in shape and counts of structures. The hemipenes of *R.* sp. nov. a (Fig. 3A) and *R. leucosticta* (Fig. 3C) are fully everted and expanded, whereas the lobes of *R.* sp. nov. b (Fig. 3B) are partially everted and expanded. The organs of the three taxa are comparable in length with 5.8 mm in *R.* sp. nov. a, 3.9 mm in *R.* sp. nov. b and 5 mm in *R. leucosticta*, reaching between 3.5 and 5 subcaudals. Hemipenial body is roughly globose in *R. leucosticta* and *R.* sp. nov. b, whereas it is cylindrical in *R.* sp. nov. a. The lobes are reduced in the three taxa, although distinctly detached from the body (bicapitate) in *R.* sp. nov. a and weakly capitate in *R. leucosticta* and *R.* sp. nov. b. In all taxa the apex of the lobes is divided into three distinct projections; the specimen of *R. leucosticta* presents a distinctly enlarged projection, originating at the asulcate face of each lobe. Sulcus spermaticus is shallow, running medially through the sulcate face, dividing into two branches at the lobular crotch and then running through the medial faces of the lobes. An extensive nude area flanks the sulcus on each side. Basis of the asulcate face of the hemipenis is nude, with no medioproximal asulcate flounces. The asulcate face and the laterals present series of equidistant flounces, each one bearing a single calcified and roughly hook-shaped spine directed towards the basis of the organ. Those flounces and spines are differentially developed within the three taxa analysed: *R. leucosticta* has less developed flounces, with reduced spines; *R.* sp. nov. b has flounces and spines moderately developed; and *R.* sp. nov. a bears remarkably developed flounces and spines, with a distinct enlarged medial hook-shaped spine in each lateral. The specimen of *R.* sp. nov. b has 20 flounces, whereas the specimens of *R.* sp. nov. a and *R. leucosticta* have 26 flounces, organized in a U-shape on the laterals of the organ.

Downloaded from https://academic.oup.com/zoolinnean/article/190/1/271/5716277 by guest on 25 April 2024

Figure 3. Sulcate (left) lateral (centre) and asulcate (right) faces of the hemipenes of *Riolama* spp.: A, *R. grandis* (RGZ 12174); B, *R. stellata* (USNM 284491); C, *R. leucosticta* (PK 2109).

THERMAL BIOLOGY

The voluntary thermal maxima (VTM) obtained for *Riolama* sp. nov. a *sensu* McDiarmid *et al.* (1988) (32.6 °C and 34.1 °C, obtained for MTR 40 266 and MTR 40 269, respectively) are similar to forest gymnophtalmids living at the base of Pico da Neblina (A. Camacho, unpublished data). This measurement is known to vary little intraspecifically (Camacho *et al.*, 2018; Wiens *et al.*,

Downloaded from https://academic.oup.com/zoolinnean/article/190/1/271/5716277 by guest on 25 April 2024

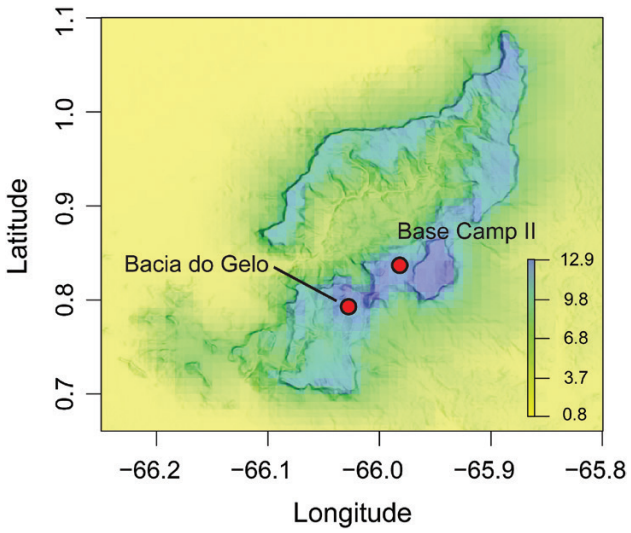

Figure 4. Thermal raster of Neblina highlands depicting the difference between the voluntary thermal maximum of *Riolama grandis* and the mean maximum air temperatures registered at the hottest month (November) over 20 years. Positive values indicate that air temperatures do not reach the maximum voluntary temperature tolerated by the lizards, even in the lowlands.

2019) and allows identification of thermal restrictions on habitat use and distribution of other gymnopthalmids (Recoder *et al.*, 2018). It thus allows a preliminary approximation of how thermal tolerances restrict the distribution of *Riolama* species. The raster of thermal safety margins shows positive values extending down into the lowlands (Fig. 4), which suggests that maximum air temperatures in lowlands should not restrict the colonization of lowlands by this species.

Molecular phylogeny and genetic distances

Our Bayesian phylogenetic tree recovers a monophyletic *Riolama* where the two new species are the sister-group of a clade formed by the other two known species, with high support (Fig. 5). The analysis recovers *R.* sp. nov. a and *R.* sp. nov. b *sensu* McDiarmid *et al.* (1988) as sister-species, while *R. leucosticta* and *R. inopinata* are recovered as closest relatives, with strong support for all nodes (PP = 1.0). Riolaminae (represented by *Riolama* spp.) was recovered as sister to the ancestor of all other Gymnophthalmidae tribes, but with weak support (PP = 0.74). The analysis also recovers Alopoglossidae and Gymnophthalmidae as sister groups and recovers strong support for the monophyly of both families (PP = 1.0).

Uncorrected net mean genetic distances for mtDNA between species of *Riolama* are presented in Table 2. Genetic distances (16S/*ND4*) range from 0.05 to 0.17 between *R. leucosticta* and *R. inopinata* (lowest), and from 0.09 to 0.24 between *R.* sp. nov. a and *R. inopinata* (highest).

Divergence times

Divergence time estimation using BEAST (Fig. 6) infers that the two new species of *Riolama* from Serra da Neblina diverged in the Early Miocene, around 16.2 Mya [median value; 95% highest posterior density interval (HPD) = 10.83–22.03 Mya]. The most recent common ancestor (MRCA) of these two species diverged from the MRCA of *R. inopinata* and *R. leucosticta* during the Oligocene, at around 27.9 Mya (HPD = 20.62–36.02 Mya); this estimate corresponds to the crown-age of *Riolama*. Riolaminae diverged from the MRCA of the Rachisaurinae and Gymnophthalminae during the mid-Palaeocene, around 60.2 Mya (HPD = 50.02–70.79 Mya). Gymnophthalminae species share a MRCA in the Eocene at around 38.8 Mya (HPD = 31.82–46.62 Mya), while the MRCA of all Cercosaurinae was dated as 60.7 Myr old (HPD = 50.63–71.35 Mya). Major estimations of divergence times retrieved within Gymnophthalmoidea (*sensu* Goicoechea *et al.*, 2016) are presented in Table 3.

Taxonomic accounts

Riolama grandis Recoder *et al.*, sp. nov.

(Figs 7–9)

Riolama sp. nov. a, McDiarmid *et al.*, 1988: 669.
Riolama sp. A (Neblina), McDiarmid & Donnelly, 2005: 515, 540; Kok, 2015: 501, fig. 7.

LSID: urn:lsid:zoobank.org:act:2EAC3B84-3D77-4EA0-B8BB-8FB2B46C0D6D

Holotype: MZUSP 116620 (field number MTR 40320; Figs 7, 8A, 9A), an adult male from 'Bacia do Gelo', in the highlands of the Serra da Neblina, Parque Nacional do Pico da Neblina, Santa Isabel do Rio Negro, Amazonas State, Brazil (0°47'37"N, 66°01'25"W; 2.013 m a.s.l; datum WGS84); collected on 18 November 2017 by M. T. Rodrigues, A. Camacho, F. Dal Vechio, I. Prates, J. M. Ghellere, R. Recoder and S. Marques-Souza.

Paratopotypes: Seven individuals, two adult males, MZUSP 116622, 116626 (field number MTR 40302, 40314), two adult females, MZUSP 116621, 116623 (field numbers MTR 40269, 40304) and three subadult females, MZUSP 116624, 116625, 116627 (field numbers MTR 40308, 40310, 40373), from the same locality as the holotype, collected between 18 November and 22 November 2017, by the same collectors as the holotype.

Downloaded from https://academic.oup.com/zoolinnean/article/190/1/271/5716277 by guest on 25 April 2024

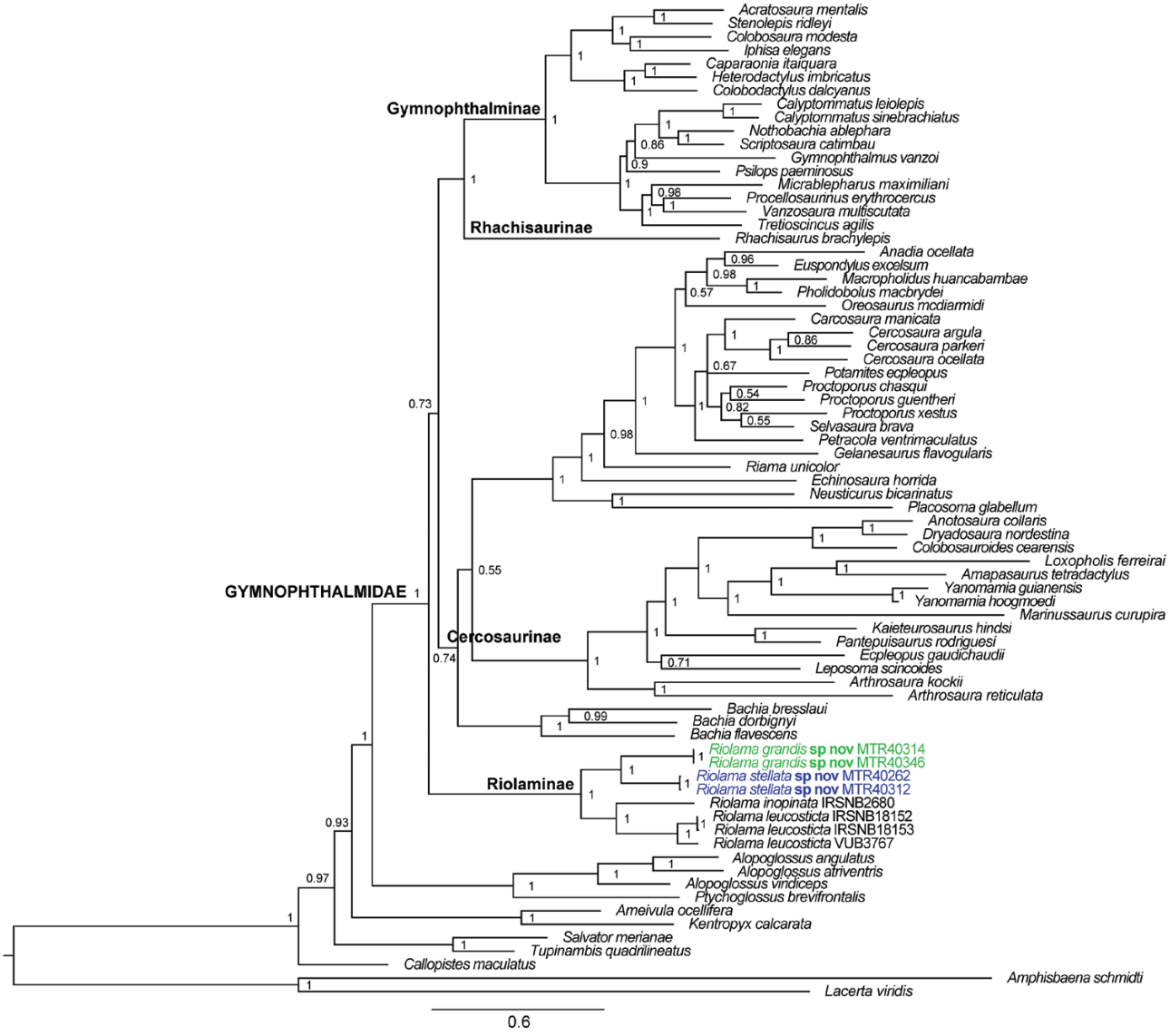

Figure 5. Bayesian phylogenetic tree based on the concatenated data set (12S + 16S + *Cytb* + *ND4* + *c-mos* + *ntf3*; 3418 bp). Node values represent Bayesian posterior probabilities, with values above 0.95 considered as high statistical support for clades.

Table 2. Mean net genetic distances (uncorrected p) among species of *Riolama* included in this study for 16S (upper right) and *ND4* (lower left)

	R. grandis	*R. stellata*	*R. leucosticta*	*R. inopinata*
R. grandis		0.066	0.062	0.089
R. stellata	0.199		0.071	0.074
R. leucosticta	0.189	0.192		0.052
R. inopinata	0.237	0.208	0.173	

Paratypes: AMNH R-178714 (field number RGZ 12174), an adult male from Camp II, 3.5 km northeast of Pico Phelps (= Pico Neblina), Cerro de la Neblina, Departamento Río Negro, Territorio Federal Amazonas, Venezuela (00°50'00" N, 65°58'48" W; 2100 m a.s.l.), collected by Richard G. Zweifel on 25 February

Downloaded from https://academic.oup.com/zoolinnean/article/190/1/271/5716277 by guest on 25 April 2024

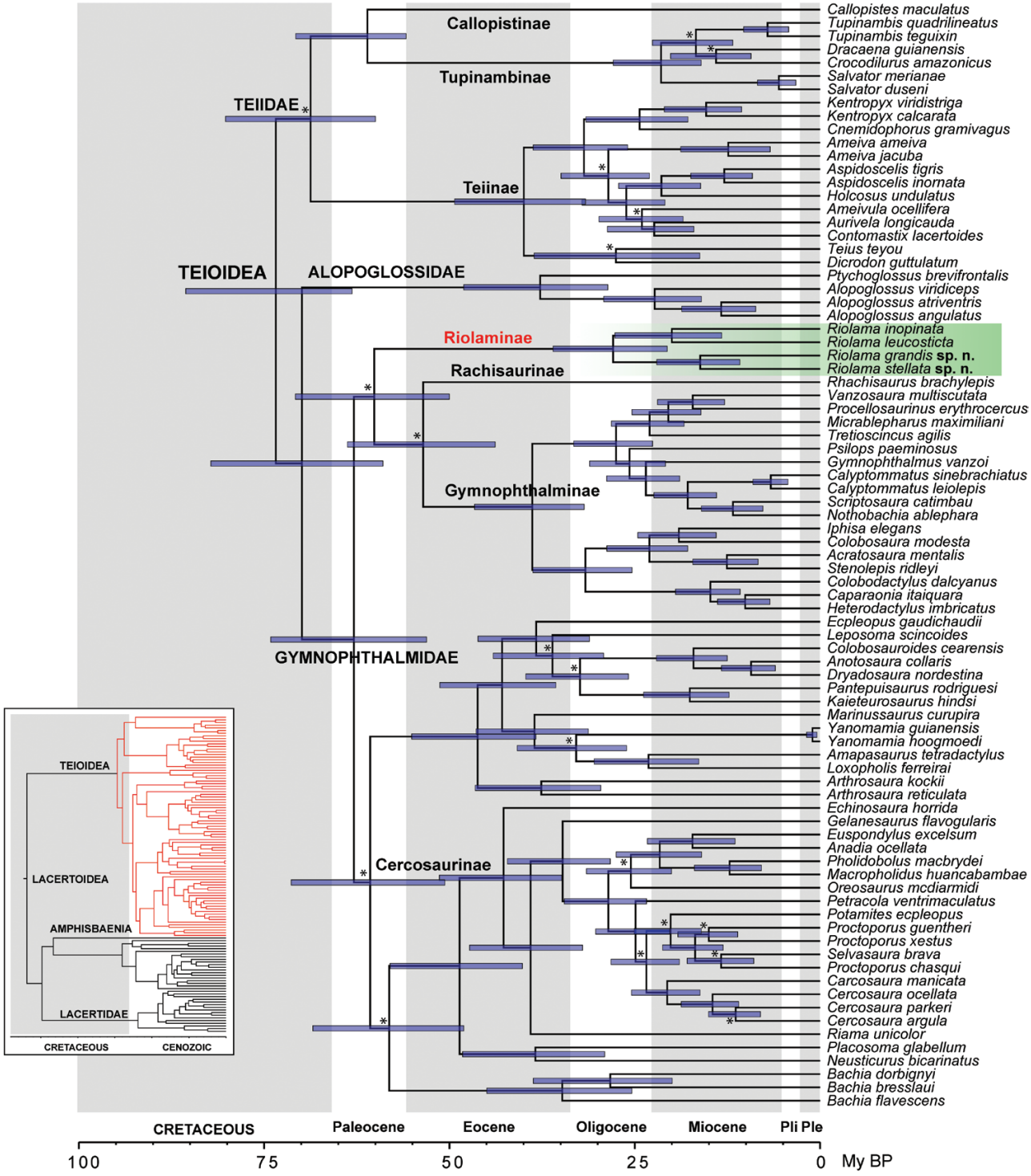

Figure 6. Time-calibrated Bayesian tree for Lacertoidea estimated using BEAST 1.10. Nodes with posterior probabilities < 0.95 are highlighted with asterisks. Representatives of *Riolama* are highlighted in green.

1984; USNM 284488 (RWM 17682), an adult female, Camp II, 3.5 km north-east of Pico Phelps, Cerro de la Neblina, Departamento Río Negro, Territorio Federal Amazonas, Venezuela (00°50'12"N, 65°58'48" W; 2.085 m a.s.l), collected by Alfred L. Gardner on 31 January 1985; MZUSP 116629, 116628, two subadult females

Downloaded from https://academic.oup.com/zoolinnean/article/190/1/271/5716277 by guest on 25 April 2024

Table 3. Comparisons of the estimated timing of diversification events (Mya) within Gymnophthalmidae in this study and former studies

Study	Software / Algorithm	MRCA Gymnophthalmoidea		MRCA Gymnophthalmidae + Alopoglossidae (former Gymnophthalmidae)	MRCA Gymnophthalmidae	MRCA Gymnophthalminae	MRCA Cercosaurinae
This study	BEAST / ucld	73.4		69.9	62.9	38.8	60.7
Zheng & Wiens, 2016	treePL / PL	94.0		89.4	79.4	53.3	76.3
Pyron & Burbrink, 2014	r8s / PL	86.3		81.3	73.7	50.1	69.9
Mulcahy *et al.*, 2012	r8s / PL	80.0		78.0	68.0	-	-
Mulcahy *et al.*, 2012	BEAST / ucld	75.0		68.0	48.0	-	-
Wiens *et al.*, 2006	r8s / PL	99.0		99.0	90.0	57.0	-
Difference between average age estimated with PL and this study		16.4		17.0	14.9	14.7	12.4
Difference between age estimated with BEAST (i.e. Mulcahy *et al.*, 2012) and this study		1.6		-1.9	-14.9	-	-

(field numbers MTR 40266, 40346), from 'Base Velha', Serra da Neblina, Parque Nacional Serra da Neblina, Santa Isabel do Rio Negro, Amazonas State, Brazil (0°46'34"N, 66°00'57"W; 2010 m a.s.l.).

Etymology: The specific epithet, *grandis*, is a Latin adjective, meaning 'big' or 'large', in reference to the larger body size of this new species compared to congeners.

Diagnosis: Following the generic diagnosis of Uzzell (1973), and comments by D. M. Harris and R. W. McDiarmid in Myers & Donnelly (2001), the new species is attributed to the genus *Riolama* by possessing well-developed limbs with five digits; digits laterally compressed with swollen tips, claws on all digits except for the first finger; tail slightly compressed laterally in section; head scales smooth, without striations; single frontonasal and frontal, paired prefrontals and frontoparietals; dorsal scales hexagonal to rectangular, imbricate, keeled; collar fold distinct; tympanum heavily pigmented and weakly depressed; oblique plicae rather than papillae on the posterior surfaces of the tongue. Additionally, the generic allocation is corroborated by molecular data.

Riolama grandis is distinguished from the remaining species of *Riolama* by the following combination of traits: (1) large size for the genus (maximum SVL 87.8 mm); (2) head long, HL 0.25 (± 0.01) times SVL; (3) dorsal scales at midbody rectangular, slightly rounded on posterior borders, slightly imbricate, weakly keeled, length 2.5–3.0 times width; (4) 30–34 transverse rows of dorsal scales; (5) 37–42 total scales around midbody: (6) eight to ten longitudinal rows of ventral scales; (7) 19–23 transverse rows of ventral scales; (8) 30 or more temporal scales; (9) seven to nine supralabials on each side; (10) six infralabials on each side; (11) four to six scales in the occipital row; (12) six to eight scales in the postoccipital row; (13) 12–15 femoral pores on each side; (14) long limbs, HLL 0.50 (± 0.03) times SVL, when limbs appressed to trunk, tip of fourth finger overlaps hindfoot to middle of lower leg; (15) 16–21 subdigital lamellae under fourth finger; (16) 23–30 subdigital lamellae under fourth toe; (17) tongue covered by scale-like papillae on the anterior half and by chevron-like plicae on the posterior half; (18) head and body dark brown (in alcohol), generally lacking cream spots dorsally and ventrally; (19) chin grey with irregular dark blotches and two long cream marks laterally; and (20) hemipenis with laterals representing a series of roughly equidistant and remarkably developed flounces, each bearing a single spine; presence of a distinctly enlarged hook-shaped spine at the centre of the hemipenial flounces row.

Downloaded from https://academic.oup.com/zoolinnean/article/190/1/271/5716277 by guest on 25 April 2024

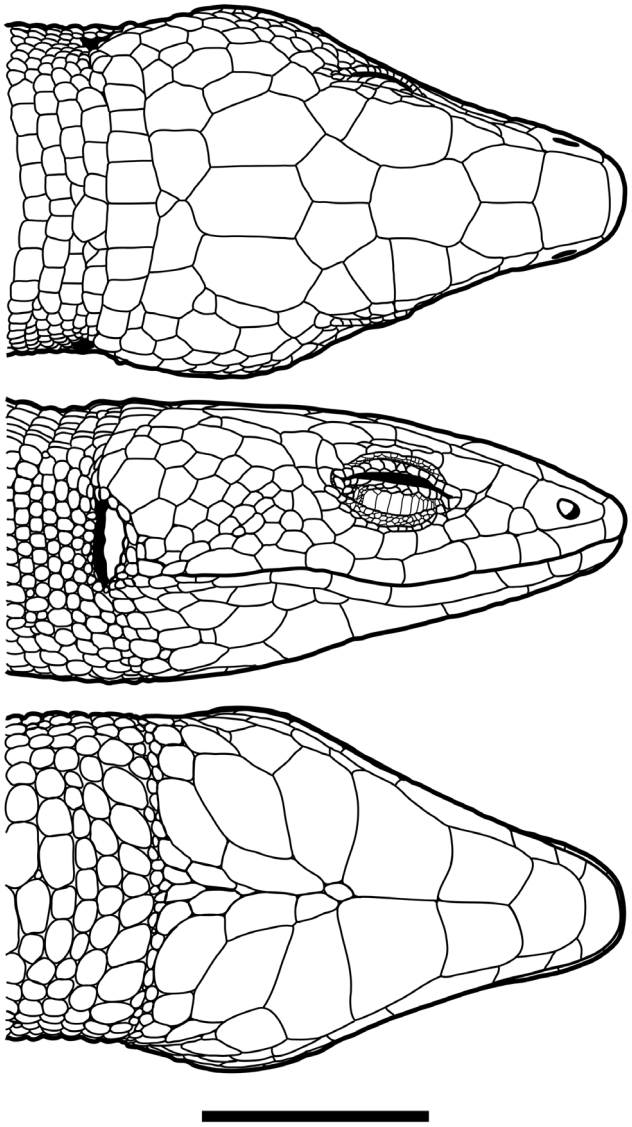

Figure 7. Dorsal, lateral and ventral views of the head of the holotype of *Riolama grandis* (MZUSP 116620, field number MTR 40320). Scale bar corresponds to 10 mm.

Description of the holotype (Figs 7, 8A): An adult male, with 87.8 mm SVL; body cylindrical, moderately stout, wider than deep; TRL corresponds to 46% of SVL. Head large, 1.56 times longer than wide, relatively distinct from neck; HL corresponds to 25% of SVL. Snout moderately broad, sides straight in dorsal view, ESD 0.39 times HL. Limbs well developed, pentadactyl with all digits clawed except for finger I. Forelimbs moderate, 29% of SVL. Hindlimbs moderately long, 46% of SVL. Tail long, two times SVL (posterior fifth regenerated), moderately robust, slightly compressed.

Head scales smooth with a few scattered sensorial pits. Rostral wider than high, visible from above; in broad contact with frontonasal (internasal), nasals and first supralabials. Frontonasal single, large, pentagonal, wider than long; in broad contact with nasals (separating nasals on midline) and prefrontals. Two large prefrontals, slightly longer than wide, shorter than frontal; in contact by a median suture about two thirds of length at margins; in contact with frontal, first supraocular and loreal. Frontal hexagonal, longer than wide, wider anteriorly; in contact with first, second and third supraoculars by a rounded suture; slightly shorter and wider than interparietal. Two large frontoparietals, pentagonal, similar in size to prefrontals, in median contact with each other by a large suture; in wide contact with frontal, third and fourth supraoculars, parietals and interparietal. Interparietal large, hexagonal, 1.6 times longer than wide, with straight margins with parietals, posterior end with a pointed border, trespassing the margins of parietals. Two large parietals, wider anteriorly; subequal to interparietal. A row of enlarged occipitals followed by a row of quadrangular postoccipitals; occipitals with five irregular scales, the median smallest and separated from interparietal by a contact between adjacent occipitals, the laterals largest, pentagonal; postoccipitals quadrangular, much larger than dorsals, the median pair largest, the laterals subsequently being smaller. Four supraoculars, first smallest, second largest, third and fourth subequal.

Nasal single, large, broadly triangular, rounder anteriorly, nostril large, ovoid, just anterior and ventral of centre of nasal, nasal without grooves; in contact with rostral, frontonasal, loreal, frenocular and a postnasal; wide contact with first supralabial, short contact with second supralabial; postnasal triangular, short, between nasal and frenocular, loreal and supralabials. Loreal quadrangular, about as high as wide, separating frenocular from nasal, in contact with prefrontal, first supraocular, first superciliary and postnasal. Frenocular pentagonal, almost as high as long, highest medially, subequal to loreal. Six subocular scales between frenocular and postocular, the fourth largest. Six superciliaries, first largest, larger than loreal, longer than high, second longer than deep, third and fourth smallest, quadrangular; the fifth quadrangular, the sixth higher than long. One row of small scales between second to fourth supraoculars and second through fifth superciliaries. One small preocular between frenocular and first superciliar. Eyelids bordered by two irregular rows of pentagonal scales and two outer rows of small granules; lower eyelid with palpebral disc covered by large opaque pentagonal scales. Temporal scales numerous (36 on the right side) smooth, hexagonal to rounded, subimbricate; increasing in size posteriorly and dorsally. Ear opening broad, ovoid, aligned vertically, partially covered by small scales. Tympanum recessed, heavily pigmented. Eight supralabials, fifth under the

Downloaded from https://academic.oup.com/zoolinnean/article/190/1/271/5716277 by guest on 25 April 2024

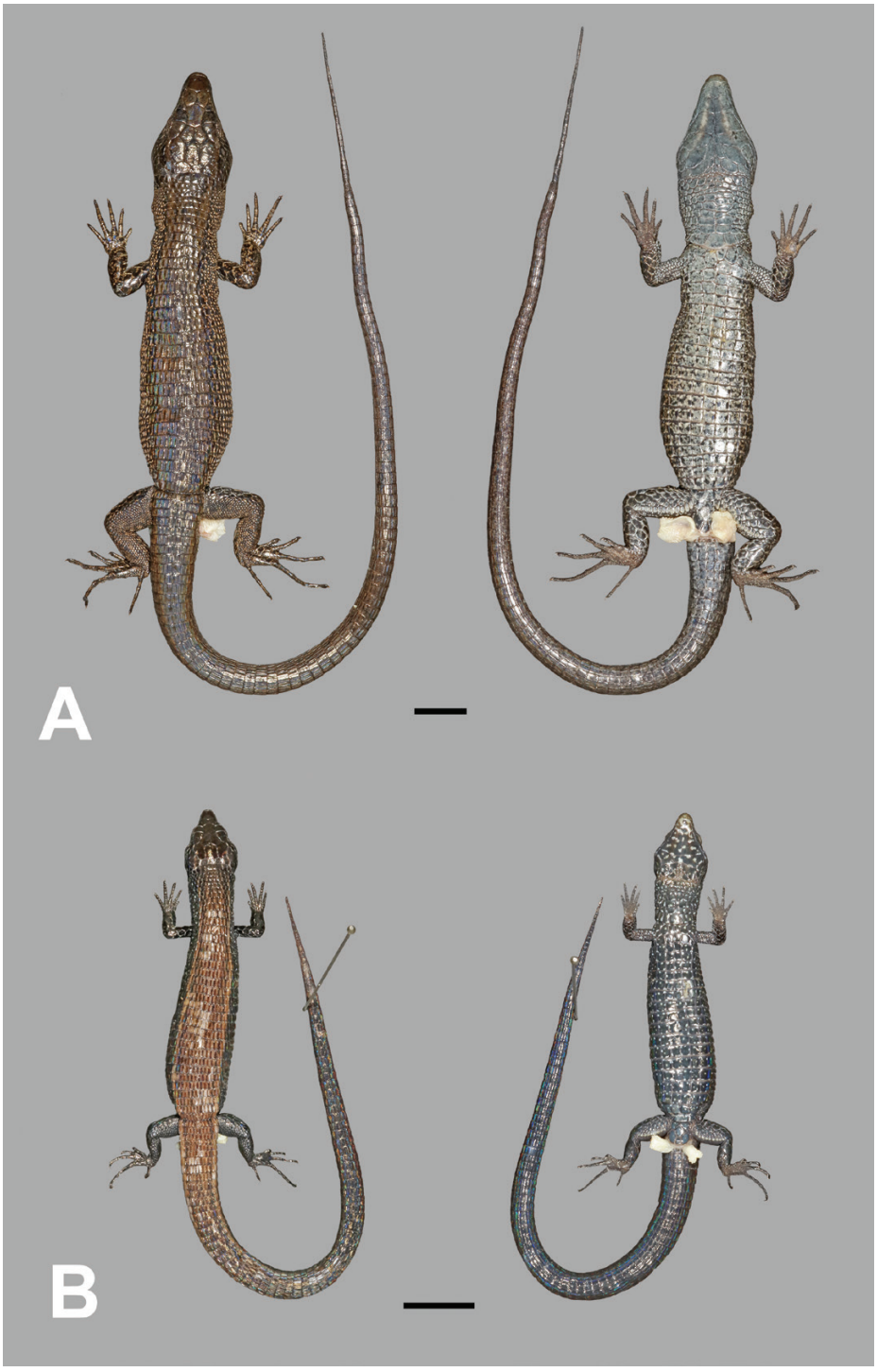

Figure 8. Dorsal and ventral views of the preserved holotype of: A, *Riolama grandis* (MZUSP 116620, field number MTR 40320); B, *Riolama stellata* (MZUSP 116616, field number MTR 40262). Scale bar corresponds to 10 mm (A) and 5 mm (B).

eye, first, fourth and seventh largest, twice longer than wide, sixth highest.

Symphyseal scale wider than long, followed by a larger and undivided pentagonal postsymphyseal contacting the first two infralabials. Six infralabials on each side, third longest. Five pairs of mentals; first three pairs contacting the infralabials laterally; first and second contacting each other medially in a straight suture; first pair

Downloaded from https://academic.oup.com/zoolinnean/article/190/1/271/5716277 by guest on 25 April 2024

Figure 9. Individuals of *Riolama grandis* in life. A, holotype (MZUSP 116620, field number MTR 40320) an adult male with 87.8 mm SVL; B, paratopotype (MZUSP 116626, field number MTR 40314), adult male with 74.7 mm SVL; C, paratype (MZUSP 116629, field number MTR 40266), a juvenile male with 41.0 mm SVL.

smaller, almost quadrangular, second pair largest and quadrangular, third pair much wider than long, almost pentagonal; third pair separated from infralabials by a row of elongated scales, the posterior two pairs separated from the infralabials by a series of large, irregular lateral scales, and separated from each other anteriorly by

Downloaded from https://academic.oup.com/zoolinnean/article/190/1/271/5716277 by guest on 25 April 2024

two large irregular scales and posteriorly by a series of small ovoid scales projected anteriorly. A distinct ventral groove between ear openings, slightly arched anteriorly, composed of an irregular row of granular scales. Collar distinct, anterior to pectoral scales, with seven scales in a single row; the median one pentagonal and largest, the remaining ones quadrangular and decreasing in size laterally. Collar fold distinct, filled with rounded, widely spaced, granular scales in six irregular rows; posterior border of medial collar scales partially overlapping anterior pectoral scale row. Gulars arranged in nine irregular transverse rows (including collar); rounded, wider than long, smaller anteriorly, increasing in size posteriorly; the five posterior rows of gulars with central scales widened, quadrangular, much larger than laterals. Sides of neck with small, subequal, subimbricate, pebble-like scales.

Dorsal scales arranged in transverse rows; first six rows with quadrangular or hexagonal scales, smooth; remaining dorsal scales on body and near tail more elongate, rectangular, imbricate, with slightly rounded posterior borders, keeled; keel on dorsal scales straight, not strongly marked; 34 transverse rows of dorsal scales between postoccipitals and posterior insertion of hind limbs; a total of 40 longitudinal rows of midbody scales (including 16 dorsal rows, six to eight lateral rows and ventrals); dorsal caudal scales similar to those on body, progressively loosing keels laterally. Transverse rows of dorsal body scales divided into two or three rows of nearly rounded lateral scales at midtrunk; anterior and posterior third of the area between limbs covered by small scales irregularly arranged; weak keels on more dorsally located lateral trunk scales; scales granular near insertion of forelimb.

Pectoral scales in two rows of seven/four scales laterally, one row of three scales medially; middle scale of three medial ones smaller than lateral ones. Ventral scales quadrangular, in 21 transverse rows and ten longitudinal rows at midbody; six scales in pre-anal shield in two rows, middle scale of anterior row large and quadrangular, lateral scales ovoid and reduced, middle scale of posterior row smaller than lateral scales which are subequal to middle scale of anterior row.

Arm covered dorsally and posteriorly with large, smooth scales; ventral surface of upper arm and inner surface of forearm with granular scales; flattened scales on surface of hand; five depressed fingers, four with claws, thumb clawless; tip of each finger slightly compressed; three scales on dorsal surface of thumb, six on second digit, eight on third, nine/ten on fourth and six/seven on fifth; dorsal scale of penultimate phalanx enlarged on all digits; five ventral scales, including one tubercle, on first digit, eleven on second, sixteen on third, 18/19 on fourth and 11 on fifth; two thenar tubercles in row with thumb tubercle along edge of hand; surface of palm covered with granular scales, some with central depressions; single, rounded, relatively protuberant outer tubercle at base of palm; fourth finger longest, followed in decreasing order by third, second, fifth and first.

Upper leg covered by large, flat scales on anterior surface; more dorsally situated scales granular, weakly keeled scales on dorsal and posterior surfaces of thigh; granular scales, some weakly keeled, on anterior and posterior surfaces of lower leg; ventral surface covered with large, flat scales. Femoral pores 14/14, some scales with one to four grooves extending to scale margins, especially on distal ones. Foot with large, flat scales dorsally; five digits, all clawed; first toe with three dorsal scales, second with seven, third with 11, fourth with 15/16, and fifth with ten, few divided; first toe with eight subdigital lamellae, second with 13/14, third has 19/20, fourth has 26/27 and fifth has 18/17, some partially or completely divided; small, granular scales on sole, some with central depressions.

Dorsal surface of tongue covered with many small scales on anterior half and chevron-shaped plicae on posterior half. Four infralingual plicae, slightly swollen, forming acute angle on midline, decreasing in size posteriorly. Maxilla and premaxilla with 24 bicuspid teeth on each side; teeth slightly curved, anterior cusps lower than posterior ones. Each dentary with 21 bicuspid teeth.

Colour of holotype: In alcohol, dorsum brown with a pair of faded light dorsolateral stripes, two to three dorsal scales wide, beginning on parietals and extending to base of tail, poorly defined on tail (Fig. 8A); a dark stripe, marginal to dorsolateral stripes; vertebral area between stripes mixed brown and dark brown; head dark brown with irregularly defined darker spots; temporal region and posterior supralabials brown mixed with dark grey; mental and inner sides of mandibular, gular and pectoral region whitish, spotted with bluish grey; outer edges of mandibles, gular and pectoral region, and ventral surfaces of body, limbs and tail bluish grey with scattered dark blotches (Fig. 8A); flanks greyish brown, each scale primarily dark; area around femoral pores and vent, beneath upper arms, and on ventral surfaces of hands and feet cream with dark mottles.

In life (Fig. 9A), background colour copper brown, dorsolateral stripes conspicuous; dorsolateral lines ochre anteriorly and brown posteriorly, black vertebral spots; head dark brown, chin and gular area cream with two transverse whitish stripes, chest and venter cream olive with black spots irregularly arranged; lateral scales black with yellowish tips; pre-anal region yellowish with black spots, black spots on legs; iris olive-cream. Lateral colour pattern extends dorsally and is visible from above. In preservative, background colour dark brown, dorsolateral stripes

Downloaded from https://academic.oup.com/zoolinnean/article/190/1/271/5716277 by guest on 25 April 2024

less conspicuous, lateral colour darker than dorsal, with yellowish dots. Ventral colour bluish grey.

Measurements of the holotype (in mm): SVL 87.8; TRL 40.8; HH 10.4; HW 14.1; HL 22.0; ESD 8.6; FEM 14.2; TIB 13.0; FTL 19.4; HUM 9.2; HAL 19.8; TAL 179.0.

Variation: The paratypes present variation in all scale counts except number of infralabials (Table 4). Temporals vary between 30 and 40; occipitals four to five (one individual with 7) and postoccipitals six to eight. Body size does not differ significantly between sexes (ANOVA, $F = 3.73$, $P = 0.10$). Males have proportionally larger FEM (ANCOVA, $F = 8.33$, $P < 0.05$) and HUM (ANCOVA, $F = 8.55$, $P < 0.05$), but the remaining morphometric variables do not differ significantly between sexes. Maxillary and premaxillary teeth vary between 20 and 25 on each dentary ($N = 6$). Colour in life is ontogenetically variable (Fig. 9B, C), with smaller individuals having a well-marked whitish bar above the eye that fades in larger specimens. Dorsal colour is lighter in smaller individuals, strongly contrasting with the lateral colour pattern. Most paratypes ($N = 6$) have well-marked black stripes medially to the dorsolateral stripes. In preservative, gular and ventral surfaces are whitish in smaller individuals but greyish in larger individuals, with light coloration restricted to white gular mottles in the larger specimens ($N = 7$). Testes of the male paratype (AMNH R-178714) are white and measure 4 mm in their largest dimension.

RIOLAMA STELLATA RECODER *ET AL.*, SP. NOV.

(FIGS 8B, 10, 11)

Riolama sp. nov. b, McDiarmid *et al.*, 1988: 669.
Riolama sp. B (Neblina), McDiarmid & Donnelly, 2005: 515, 540; Kok, 2015: 501, fig. 7.

LSID: urn:lsid:zoobank.org:act:F3552C7E-55A2-4A11-BC60-8977D050CB02

Holotype: MZUSP 116616 (field number MTR 40262; Figs 8B, 10), a male from 'Bacia do Gelo', in the

Table 4. Variation in quantitative characters (morphometrics and scale counts) in males and females of *Riolama grandis* and *Riolama stellata*

Species	*Riolama grandis*		*Riolama stellata*	
Sex	Male	Female	Male	Female
N	*N* = 4	*N* = 8	*N* = 5*	*N* = 5
SVL	77.1 ± 7.2 (72.6–87.8)	53.3 ± 14.6 (37.7–72.7)	50.3 ± 5.8 (41.9–56.4)	52.4 ± 4.9 (44.4–57.3)
TRL	36.5 ± 2.9 (34.2–40.8)	24.2 ± 8.8 (14.7–37.1)	24.5 ± 2.0 (21.8–27.1)	26.0 ± 3.9 (19.5–29.1)
HH	9.3 ± 0.7 (8.6–10.4)	5.9 ± 1.8 (4.0–8.8)	6.1 ± 1.6 (4.2–8.0)	6.3 ± 1.4 (4.7–8.3)
HW	12.3 ± 1.6 (10.3–14.1)	8.1 ± 2.0 (6.0–10.6)	7.7 ± 1.1 (6.0–8.8)	7.2 ± 0.7 (6.1–8.0)
HL	19.0 ± 2.1 (17.2–22.0)	12.8 ± 3.0 (9.9–16.5)	10.7 ± 1.8 (8.6–12.7)	10.8 ± 1.1 (9.5–11.9)
ESD	7.5 ± 0.8 (6.9–8.6)	5.2 ± 1.2 (4.1–6.8)	4.0 ± 0.7 (3.2–4.9)	4.1 ± 0.4 (3.5–4.7)
FEM	13.3 ± 0.7 (12.5–14.2)	8.9 ± 2.3 (6.2–11.9)	6.5 ± 0.8 (5.6–7.7)	6.5 ± 0.8 (5.5–7.6)
TIB	11.8 ± 0.9 (10.8–13.0)	8.3 ± 2.3 (5.7–11.1)	6.5 ± 1.0 (5.2–7.6)	6.6 ± 0.8 (5.7–7.7)
FTL	18.9 ± 0.5 (18.5–19.4)	13.6 ± 3.2 (10.4–18.0)	9.2 ± 1.3 (7.6–10.7)	9.6 ± 1.1 (8.3–10.8)
HUM	8.6 ± 0.4 (8.2–9.2)	5.6 ± 1.5 (3.8–7.4)	5.0 ± 1.1 (4.0–6.7)	4.6 ± 0.5 (4.2–5.2)
HAL	18.8 + 0.8 (17.8–19.8)	13.4 ± 3.3 (10.0–18.0)	9.0 ± 1.0 (7.7–10.2)	9.6 ± 1.0 (8.6–10.7)
TAL	178.2 ± 1.1 (177.4–179.0)	104.6 ± 39.7 (76.3–150.0)	72.4 ± 12.7 (61.0–90.4)	63.1 ± 6.3 (56.0–68.0)
TAL/SVL	2.2 ± 0.3 (2.0–2.4)	2.1 ± 0.2 (1.9–2.3)	1.5 ± 0.3 (1.2–1.9)	1.2 ± 0.04 (1.2–1.3)
DOR	31.5 ± 1.9 (30–34)	30.9 ± 0.6 (30–32)	34.8 ± 0.8 (34–36)	35 ± 2.8 (32–38)
VENT	21 ± 1.6 (19–23)	20.9 ± 0.6 (20–22)	20 ± 1.2 (19–22)	20 ± 1.6 (18–22)
GUL	9 ± 0.8 (8–10)	8.6 ± 0.5 (8–9)	7.2 ± 1.3 (6–9)	7.4 ± 0.9 (6–8)
SAM	39 ± 1.8 (37–41)	39.8 ± 1.9 (36–42)	37 ± 1.0 (36–38)	35.8 ± 2.0 (34–38)
4FL	18.3 ± 1.9 (17–21)	19.1 ± 1.6 (16–21)	11.6 ± 0.5 (11–12)	10.6 ± 1.1 (9–12)
4TL	26.5 ± 2.4 (23–28)	27.3 ± 2.4 (23–30)	17.2 ± 1.5 (15–19)	17.6 ± 0.5 (17–18)
SL	16 ± 0.8 (15–17)	16.1 ± 0.4 (16–17)	9.2 ± 3.6 (6–14)	8.2 ± 3.3 (6–14)
IL	12	12	9 ± 3.3 (6–13)	7.8 ± 2.5 (6–12)
POR	27 ± 2.2 (24–29)	27.3 ± 1.5 (25–29)	18.5 ± 0.6 (18–19)	18.3 ± 1.7 (16–20)
SAT	29.8 ± 2.9 (26–33)	28.3 ± 2.8 (23–32)	28.4 ± 3.4 (25–33)	27.7 ± 3.1 (25–31)

*MTR 40313, a juvenile (24.4 mm SVL), represent an extreme outlier in body-size and was not included in morphometric statistics.

Downloaded from https://academic.oup.com/zoolinnean/article/190/1/271/5716277 by guest on 25 April 2024

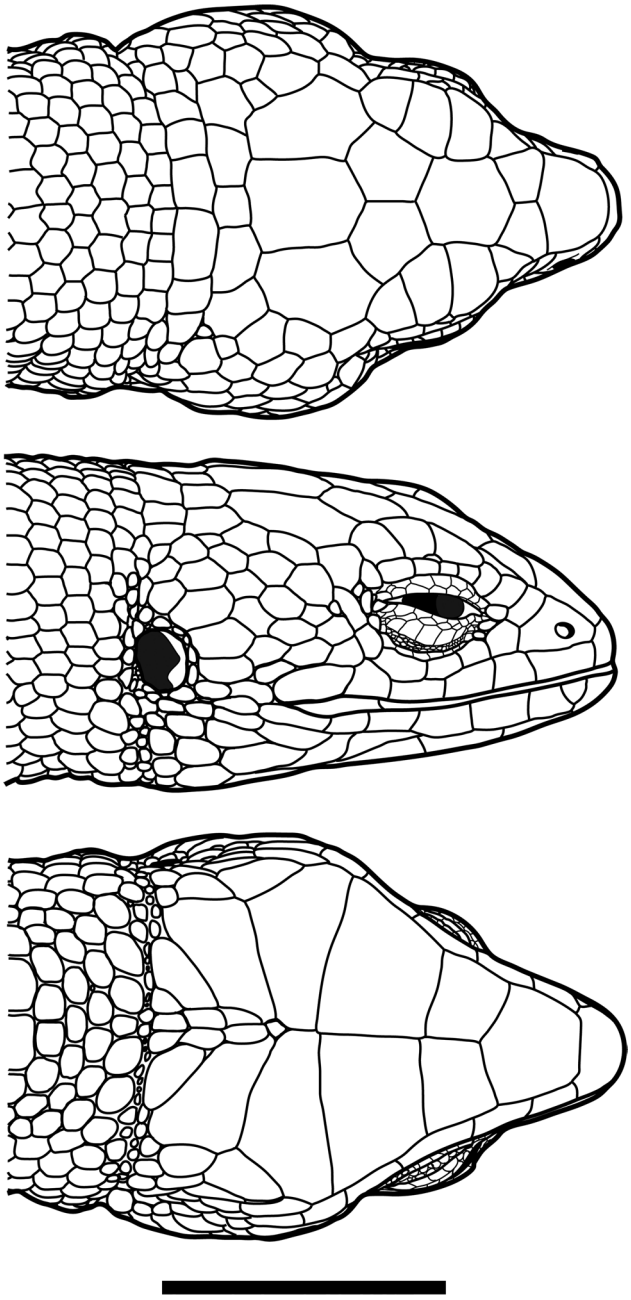

Figure 10. Dorsal and ventral views of the preserved holotype of *Riolama stellata* (MZUSP 116616, field number MTR 40262). Scale bar corresponds to 10 mm.

highlands of the Serra da Neblina, Parque Nacional do Pico da Neblina, Santa Isabel do Rio Negro, Amazonas State, Brazil (0°47'34"N, 66°01'30"W; 2000 m a.s.l., datum WGS84); collected on 18 November 2017 by M. T. Rodrigues, A. Camacho, F. Dal Vechio, I. Prates, J. M. Ghellere, R. Recoder and S. Marques-Souza.

Paratopotypes: MZUSP 116617 (field number MTR 40309) an adult male; MZUSP 116618 (MTR 40312) an adult female, and MZUSP 116619 (MTR 40313), a juvenile male, all from the same locality as the holotype (0°47'34"–0°47'37"N; 66°01'25"–66°01'33"W) collected between 18 November and 20 November 2017, by the same collectors as the holotype.

Paratypes: Five individuals from Camp II, 3.5 km north-east of Pico Phelps, Cerro de la Neblina, Departamento Río Negro, Territorio Federal Amazonas, Venezuela (00°50'12"N, 65°58'48"W; 2085 m a.s.l), USNM 284491 (field number RWM 17671), USNM 284489 (RWM 17680), collected by Alfred L. Gardner on 31 January 1985; USNM 562652 (RWM 17651), on 29 January 1985, and USNM 562653 (RWM 17659), USNM 284490 (RWM 17660), on 30 January 1985, collected by Roy W. McDiarmid; USNM 284492 (RWM 17284), from Camp II, 2.8 km north-east of Pico Phelps, Cerro de la Neblina, Departamento Río Negro, Territorio Federal Amazonas, Venezuela (00°50'00"N, 65°58'48"W; 2085–2100 m a.s.l), collected by Roy W. McDiarmid on 21 February 1984; USNM 562654 (ALG 14138), from Camp II, 2.5 km north-east of Pico Phelps, Cerro de la Neblina, Departamento Río Negro, Territorio Federal Amazonas, Venezuela (00°50'04"N, 65°58'48"W; 2085 m a.s.l), collected by Alfred L. Gardner on 20 March 1984.

Etymology: The specific epithet is the Latin adjective stellatus, which means 'starred', referring to the ventral and lateral colour pattern composed of light dots scattered on a dark background, which resemble a starry night sky.

Diagnosis: The generic diagnosis of *R. stellata* follows that presented for *R. grandis* above. *Riolama stellata* is distinguished from the remaining species of *Riolama* by the following combination of traits: (1) a small body size for the genus (maximum SVL 52.9 mm); (2) head short, HL 0.19 (± 0.01) times SVL; (3) dorsal scales at midbody slightly hexagonal, imbricate, broadly keeled, length 2.5–2.9 times width, dorsal rows clearly defined; (4) 33–38 transverse rows of dorsal scales; (5) 34–38 total scales around midbody; (6) six longitudinal rows of ventral scales; (7) 17–22 transverse rows of ventral scales; (8) 14–23 temporal scales; (9) six to seven supralabials on each side; (10) six to seven infralabials on each side; (11) five to seven scales in the occipital row; (12) five to seven scales in the postoccipital row; (13) eight to 11 femoral pores on each side; (14) short limbs, HLL 0.37 (± 0.02) times SVL, when limbs appressed to trunk, tip of fourth finger overlaps hindfoot to middle of third toe; (15) subdigital lamellae under fourth finger: 11–13; (16) subdigital lamellae under fourth

Downloaded from https://academic.oup.com/zoolinnean/article/190/1/271/5716277 by guest on 25 April 2024

Figure 11. Paratopotype of *Riolama stellata* in life (MZUSP 116617, field number MTR 40309), an adult male with 41.9 mm SVL. A, overall view; B, detail of the head.

toe: 14–19; (17) tongue surface entirely covered with plicae arranged in chevrons with anteromedial apices; (18) head and body dark (in alcohol), head dorsally and ventrally spotted with cream dots, body unspotted dorsally, ventrally black and heavily spotted with cream dots; (19) chin dark, blotched with cream marks; and (20) hemipenis with laterals consisting of a series of roughly equidistant and moderately developed

Downloaded from https://academic.oup.com/zoolinnean/article/190/1/271/5716277 by guest on 25 April 2024

flounces, each bearing a single spine; absence of the distinctly enlarged hook-shaped spine at the centre of the hemipenial flounces row.

Description of the holotype (Figs 8B, 10): An adult male, with 47.2 mm in SVL; body cylindrical, elongate, wider than deep. TRL corresponds to 53% of SVL. Limbs short but well developed, limbs pentadactyl with all digits clawed except for finger I. Forelimb 24% of SVL and hindlimb 37% of SVL. Tail slightly flattened laterally in section, about 1.9 times the SVL. Head short, 1.2 times longer than wide, HL 0.19 times SVL, only slightly differentiated from neck; snout short, ESD 0.37 times HL.

Head scales smooth with scattered sensorial pits, more numerous on anterior region. Rostral wider than high, visible from above; broad contact with frontonasal. Frontonasal large, single, pentagonal, longer than wide, slightly wider posteriorly, wider and shorter than frontal, completely separating nasals. Two prefrontals, quadrangular, widest anterolaterally; in contact with each other by a median suture about half size of length at margins; in contact with frontonasal, frontal, first supraocular, thigh contact with first superciliary and loreal. Frontal hexagonal, large, slightly longer than wide, contacting first three supraoculars laterally. Two large frontoparietals, pentagonal, about 50% larger than prefrontals, contacting each other by a large suture; in wide contact with frontal, third and fourth supraoculars, parietals and interparietal. Interparietal large, pentagonal, longer than wide, with straight margins with parietals, posterior end with a straight border, coincident with margins of parietals. Two large parietals, much wider anteriorly; slightly longer than interparietal. A row of five occipitals followed by a row of six postoccipitals; middle occipital scale smaller than lateral ones, medial pair of postoccipitals larger than outers. Four supraoculars, first smallest, second largest, fourth smaller than third.

Nasal single, large, triangular, rounder anteriorly, nostril ovoid, near middle of nasal scale, nasal not grooved; in contact with rostral, frontonasal, loreal and frenocular, in wide contact with first supralabial, and short contact with second supralabial. Loreal quadrangular, two times higher than wide, in contact with frontonasal, prefrontal, first superciliary, preocular and frenocular, not contacting supralabials. Frenocular pentagonal, almost as high as long, shorter than loreal. Four subocular scales between frenocular and postocular, the third largest and extending ventrally between fourth and fifth supralabials. Seven superciliaries between loreal and posterior edge of eye, separating upper eyelid from supraoculars, first two largest. A single, small scale situated between second and third supraoculars and fourth and fifth superciliaries. One small preocular between frenocular and first superciliary. Eyelids bordered by a single row of small granules on upper eyelid and two irregular rows at lower eyelid; lower eyelid with palpebral disc covered by large opaque pentagonal scales. Twenty smooth temporal scales, hexagonal to rounded and subimbricate; increasing in size posteriorly and dorsally. Ear opening broad, ovoid, aligned vertically. Tympanum moderately recessed, heavily pigmented. Six supralabials, fourth under the eye, first and sixth largest, two times longer than wide, fifth highest.

Symphyseal scale wider than long, followed by a larger and undivided pentagonal postsymphyseal contacting the first two infralabials. Six infralabials on each side, first longest. Five pairs of mentals; first three pairs contacting the infralabials laterally, contacting each other medially in a straight suture; first pair smaller and almost quadrangular, second pair largest and quadrangular, third pair much wider than long, almost pentagonal; posterior two pairs separated from infralabials by a series of large, irregular lateral scales, and from each other by two rows of elongate scales projected anteriorly. A distinct groove between ear openings, separating mentals from gulars, composed of an irregular row of granular scales. Collar distinct, anterior to pectoral scales, consisting of a row of seven enlarged rectangular scales between anteromedial insertions of forelimbs; medial scale largest and more quadrangular than others; collar fold distinct, with rounded, widely spaced, granular scales in two irregular rows. Gular scales arranged in eight transverse rows (including collar); anterior four transverse rows of gulars with subequal scales; posterior rows of gulars with paramedian scales presenting two longitudinal rows of greatly enlarged rectangular gulars, larger posteriorly. Lateral scales on neck roughly quadrangular, slightly protuberant; scales between the lateral extension of collar and forelimb small, granular.

Dorsal scales arranged in transverse rows; first six rows with hexagonal scales, as wide as long, imbricate, smooth; remaining dorsal scales on body and near tail more elongate, hexagonal, more than two times longer than wide, more imbricate and keeled posteriorly; keels broad; dorsal scales not forming longitudinal rows; 34 transverse rows of dorsal scales between postoccipitals and posterior insertion of hind limbs; 38 longitudinal rows of midbody scales (including 16 dorsal rows, eight lateral rows each side and ventrals); dorsal caudal scales similar to those on body, progressively loosing keels laterally. Lateral scales progressively smaller than dorsals towards venter; nearly rectangular at mid-trunk, imbricate, divided into two occasionally three rows per dorsal row; granular scales irregularly arranged over about a third of the lateral area between limbs; weak keels on more dorsally located lateral trunk scales; scales granular near insertion of hind limb.

Downloaded from https://academic.oup.com/zoolinnean/article/190/1/271/5716277 by guest on 25 April 2024

Pectoral scales in two rows, ten scales in anterior row and seven in posterior one. Ventral scales quadrangular, in 18 transverse rows and six longitudinal rows at midbody; six scales in pre-anal shield in two rows, anterior middle scale largest, pentagonal, bordered laterally by anterior and posterior pair of about equal size and posteromedially by a small quadrangular scale.

Forelimb covered dorsally and posteriorly with large, smooth scales on anterior and posterior surfaces of upper arm and forearm; ventral surface of upper arm covered with granular scales; hands covered dorsally with flattened, quadrangular plates; five short fingers, thumb reduced and clawless, four other digits clawed, depressed, with compressed tip; two scales on dorsal surface of thumb, five on second digit, six on third, seven on fourth and five on fifth; thumb with three subdigital lamellae, basal one in form of keeled tubercle, other two flattened; second digit with eight ventral scales, third with nine/ten, fourth with 12 and fifth with seven, most undivided, all flattened; two additional tubercles in row with basal thumb tubercle along border of palm; palm covered by granular scales, some with central depressions; slightly rounded, protuberant tubercle located on posterolateral border of palm; fourth digit longest, followed in decreasing order by third, second, fifth and first.

Hindlimbs covered on anterior and dorsal surfaces of thighs with large scales, generally smooth, few slightly keeled; scales on posterior surface of thigh small, granular; scales on ventral surface rounded; scales on ventral surface of lower leg large, smooth, those on dorsal surface smaller, some weakly keeled, becoming granular near foot. Femoral pores nine/nine, with one to three grooves extending to scale margins. Feet covered dorsally by large flattened scales; five short digits, all clawed; scales on dorsal surface of toes smooth, numbering three on first toe, five on second, eight on third, ten on fourth and six on fifth; five subdigital lamellae on first toe, seven on second, 12 on third, 14 on fourth and nine on fifth, some scales partially or completely divided; four semicircular tubercles on inner edge of basal lamellae on third toe; scales on sole of foot small, granular, often with central depression.

Tongue surface entirely covered with plicae arranged in chevrons with anteromedial apices; some plicae divided, especially posteriorly, into fragments of variable length. First infralingual plicae distinct, long and pointed; other three rounded and meeting in acute angle on midline. Eighteen teeth on each side of upper jaw; anterior ones curved and primarily unicuspid, posterior ones more erect and bicuspid; posterior cusp much higher than anterior one. Mandible with seventeen teeth on each side; morphology similar to maxillary teeth.

Colour of holotype: Background coloration in life is dark brown on dorsum and black on ventral, lateral, gular and mental regions (Fig. 11). Dull orange-brown dorsolateral stripes extending to the tail, dorsally bordered by faded black parallel stripes. Black surfaces with several small whitish blotches. Limbs black with small whitish blotches on dorsal and ventral surfaces. Tail dark brown. Colour in preservative (Fig. 8B) is similar, face and dorsal surface of head dark brown with many small, rounded, cream spots, somewhat poorly defined; lower mandible and gular region grey, slightly bluish, with small, irregular whitish spots; dorsum dark brown with irregular light brown dashes, no rounded dots; longitudinal, dorsolateral cream stripe, 0.5 to 2.5 scales wide extending from occipital scales on head to posterior part of tail, less distinct on tail; dorsally tail dark brown with light brown dashes; sides blackish brown with many small, rounded, cream or whitish dots on all transverse scale rows; ventral surfaces of body, forelimbs, hindlimbs and tail lead-grey and marked with many, small rounded whitish spots; venter slightly yellowish anteriorly; one to four spots on each ventral scale, ventral spots larger than lateral ones; pattern on pre-anal shield similar; spots on ventral surface of tail more scattered and considerably smaller than those on other parts of venter; fore- and hindlimbs, including toes, blackish brown with white or cream dots similar to sides; palms and soles greyish, without spots.

Measurements of the holotype (in mm): SVL 47.2; TRL 24.9; HH 5.0; HW 7.3; HL 9.1; ESD 3.4; FEM 6.2; TIB 5.7; FTL 8.2; HUM 4.4; HAL 8.8; TAL 90.4.

Variation: The type series shows some variation in quantitative morphological traits, as presented in Table 4. Temporals vary between 14 and 23; occipitals five to seven; postoccipitals five to seven (Supporting Information, Table S2). Sexes do not differ significantly in size (ANOVA, $F = 0.38$, $P = 0.55$), but males are proportionally larger in HW than females (ANCOVA, $F = 19.80$, $P > 0.01$).

Additionally, the following morphological traits show some variation among the paratypes when compared to the holotype: right prefrontal smaller than left ($N = 1$); posterior fifth of right frontal separated into second scale ($N = 1$); frontal and left frontoparietal fused, replaced by anomalous crenulate scale sutures ($N = 2$); a weakly defined depression (similar to nasal groove) from nostril to supralabial scale ($N = 4$); four or six subocular scales ($N = 5$); six superciliaries ($N = 4$); seven or eight scales on lower border of upper eyelid ($N = 9$); six or seven scales on upper border of lower eyelid ($N = 6$); four to six scales in middle of palpebral disc ($N = 6$); seven supralabials on left side ($N = 2$); seven infralabials ($N = 1$); three pairs of chin shields,

Downloaded from https://academic.oup.com/zoolinnean/article/190/1/271/5716277 by guest on 25 April 2024

sometimes three pairs and one shield on only one side (N = 5); seven, eight or ten scales in collar (N = 7); 12 or 13 scales in anterior pectoral scale row (N = 9); pre-anal shield of seven to ten scales (N = 12); tongue plicae divided or not, or with large number of scales, especially on middle part (N = 11); 18 (N = 2) to 19 (N = 1) teeth on each side of upper jaw; mandible with 17 (N = 2) to 18 (N = 1) teeth on each side.

In life, paratypes are dorsally dark brown, but dorsolateral stripes fade to pale brown in some adult males, and in all females and juveniles. Dark brown marks occur between dorsolateral lines in larger individuals. Light longitudinal body stripes may begin on first or fourth supraocular scales or on parietal scales; straight blackish longitudinal lines bordering light dorsolateral stripes sometimes ending mid-dorsally or extending to tail. Lateral colour deep black with white spots in adult males; dark brown with small brown spots the same colour as dorsolateral lines in adult females and juveniles. A small juvenile (MTR 40313) has a lateral dark brown colour with light brown blotches arranged in longitudinal lines. In preservative, venter and gular regions deep black in males with well-marked white spots; in females, venter and gular regions are dark brown, with small light brown spots, light brown midventral colour and cream gular region. Ventral and gular regions in juveniles entirely cream without spots.

DISCUSSION

The Pantepui region represents a hotspot for biodiversity discoveries in South America. The high level of endemism and complex evolutionary relationships makes this a key region for biogeographical studies of the South American herpetofauna (Hoogmoed, 1979; McDiarmid & Donnelly, 2005; Kok, 2013). Due to the remoteness of the Guiana Highlands, the exploration and sampling of the Pantepui fauna has been a time-consuming and logistically challenging endeavour. A substantial part of its sampled diversity still remains to be formally described (McDiarmid & Donnelly, 2005).

Riolama and the monotypic and likewise microteiid genera *Adercosaurus* and *Pantepuisaurus* are the only known lizard groups endemic to high-elevation habitats in the Pantepui region (Myers & Donnelly, 2001; Kok, 2009). As such, these organisms have the potential to improve our understanding of the history and evolution of the biota of the tepuis. The recognition of two new species of *Riolama* in this work increases the diversity of the genus to six species and provides new elements to understand the morphological variation and distribution patterns in the genus.

The two new species from the Neblina tepui are distinct from congeners in their external morphology (Supporting Information, Table S2). *Riolama grandis* differs from all other four species of the genus (comparative combined values in brackets) by its larger body size, with maximum SVL 87.8 mm (42.8–58.9 mm); its longer head, with HL 25% of SVL (19–23%); its longer hindlimbs, with HLL around 50% of SVL (37–43%); the presence of rectangular dorsals at midbody (hexagonal or pentagonal); more than 29 temporals (less than 24); larger number of subdigital lamellae, with more than 15 lamellae under fourth finger (less than 15) and more than 22 lamellae under the fourth toe (less than 21); and the anterior portion of the tongue is covered by papillae (by plicae anteriorly).

Riolama stellata can be readily diagnosed from *R. grandis*, *R. luridiventris* Esqueda *et al.*, 2004 and *R. uzzelli* Molina & Señaris, 2003 by a smaller body size, with maximum SVL 52.9 mm (57.6–87.8 mm) and a ventral pattern with well-defined, whitish spots on a black background (greyish to brownish ventral colour without spots). *Riolama stellata* can be diagnosed from *R. leucosticta* and *R. inopinata* by the presence of 33–38 dorsals (28–33); 34–38 scales around midbody (26–30); and tongue uniformly covered by plicae (covered by plicae but interrupted by papillae medially).

The strong disparity in body-size, shape and colour between the two new syntopic species of the Neblina is remarkable. Both species were found in sympatry in similar habitats, and differences in microhabitat use consisted of a higher propensity of *R. grandis* to climb on low vegetation, while *R. stellata* is exclusively found on the ground. The co-occurrence of congeneric lizards in the Pantepui region is rare (Esqueda *et al.*, 2004; McDiarmid & Donnelly, 2005; Kok, 2015). Thus, the morphological and apparent niche differences between the two *Riolama* species may allow its coexistence in the Neblina range by minimizing competition, a hypothesis that remains to be tested with further observations.

The restriction of *Riolama* to high elevations is supported by our relatively large series obtained at the plateau, despite the absence of individuals in the well-sampled lowland rainforests adjacent to the Neblina range. Nevertheless, our empirical data on the thermal tolerance of *Riolama grandis* suggest that maximum yearly temperatures do not constrain their distribution to the highlands. This result is consistent with patterns emerging in other mountain lizards, within (Strangas *et al.*, 2019) and outside the tropics (Wiens *et al.*, 2019), that suggest that maximum temperatures are not a major factor limiting lizard species to mountain tops. These previous studies proposed that other reasons for narrow elevational ranges in upland lizards may encompass exclusion due to superior competitor species from the lowlands, a

Downloaded from https://academic.oup.com/zoolinnean/article/190/1/271/5716277 by guest on 25 April 2024

lack of appropriate microhabitats, or other behavioural restrictions that prevent the occupation of the highly diverse lower tropical forests by these lizards. This may also be the case for *Riolama* species.

Hemipenial variation in *Riolama*

The two new species also improve our understanding of the variation in hemipenis morphology in the genus. Kok (2015) described the hemipenis of *R. inopinata* and compared it to a hemipenis of *R. leucosticta*, suggesting the reduced hemipenial size of the former species as a possible diagnostic characteristic, although considering the possibility that the type specimens of *R. inopinata* represent subadults without completely developed genitalia. The hemipenes of *R. grandis*, *R. stellata* and an additional specimen of *R. leucosticta* reinforce the possibility that the typical series of *R. inopinata* is composed of subadults, considering the larger size of the hemipenes herein described (5 mm in *R. leucosticta*, 6 mm in *R. grandis*, 4 mm in *R. stellata*, versus *c.* 2 mm in *R. inopinata*). The number of flounces bearing spines in the specimens of *R. leucosticta* and *R. grandis* analysed herein are comparable with those reported by Kok (2015) for *R. leucosticta* (26 versus 28–30 in Kok's sample), whereas the number of flounces in *R. stellata* is more similar with that reported for *R. inopinata* (20 vs. 16–21).

Phylogeny and biogeography of *Riolama*

Our phylogenetic results, which include samples of the two new species of *Riolama* and an expanded set of loci, agree with previous findings that *Riolama* is monophyletic (Kok, 2015). Our analyses also support an early divergence of *Riolama* in Gymnophthalmidae (Kok, 2015; Goicoechea *et al.*, 2016), although with limited support for its phylogenetic position. In agreement with this finding, the monophyly of the different tribes within Gymnophthalmidae has been well supported in different molecular studies, but the relationships among tribes remains controversial (Pellegrino *et al.*, 2001; Castoe *et al.*, 2004; Goicoechea *et al.*, 2016).

The high molecular distance separating *R. grandis* and *R. stellata* suggests that the two species potentially diverged at a time when the Neblina Plateau was much more extensive than today (Kok, 2013). Nevertheless, the sympatric distribution and sister-relationships between *R. grandis* and *R. stellata* (phylogenetic clustering) contrasts with the high morphological disparity between the two species when compared to that of their congeners (phenotypic overdispersal), which is consistent with evolutionary change in traits associated with niche occupancy and local adaptation (Emerson & Gillespie, 2008). Therefore, whether these two species originated in the same mountain range or became sympatric after diverging in allopatry can be only speculated. The known distribution of *Riolama* is fragmentary, and we still lack molecular data for other species in the genus that may be more closely related to one of the two Neblina species to better assess biogeographical patterns.

Our Bayesian relaxed-clock analysis suggests that the onset of *Riolama* diversification dates back to the Oligocene (*c.* 28 Mya). This is the first estimate for the timing of diversification of endemic lizards of the Pantepui region, and it is comparable to estimates of the crown ages of Pantepui frogs, *Stefania* (*c.* 26 Mya; Kok *et al.*, 2016) and *Oreophrynella* (*c.* 22 Mya; Kok *et al.*, 2017). The dating matches the observations of Kok (2013), who hypothesized a period of accelerated uplift and high fragmentation during the Eocene/Oligocene (25–45 Mya), triggering diversification in the Pantepui herpetofauna. Nevertheless, some species and populations of frogs and lizards from tepui summits were isolated as recent as the Pleistocene/Holocene (Kok *et al.*, 2012; Salerno *et al.*, 2012). Therefore, these results reinforce the idea that the current tepui herpetofauna has a composite history where certain groups descend from old (pre-Pleistocene) highland species and others derived more recently from lowland ancestors, supporting the role of both vicariance and dispersal for its diversification (Hoogmoed, 1979; Kok, 2013).

Because the phylogenetic relationships among tribes within Gymnophthalmidae are not well established, our ability to make statements about the origins of *Riolama* is limited. However, considering the estimated age of the MRCA of Riolaminae and its sister lineage (Rachisaurinae + Gymnophthalminae) in the mid-Palaeocene (*c.* 60 Mya), it is likely that the group has been present on highlands in northern South America for a long period, being, together with *Ceuthomantis* (Heinicke *et al.*, 2009), possibly one of the oldest groups of Pantepui animals studied to date (Kok, 2013). The diversity in *Riolama* might not be completely known, even though new species have recently been discovered (Kok, 2015). Thus, the current diversity and distribution patterns in *Riolama*, as in other ancient groups of the Pantepui region, might have been strongly shaped by Tertiary diversification and extinctions in previously continuous tablelands that eroded into isolated tepuis, supporting the Plateau Hypothesis (Hoogmoed, 1979; McDiarmid & Donnelly, 2005). Furthermore, an old divergence time and absence of species in lowlands gives limited support to dispersal theories such as the Cool Climate Hypothesis or Habitat Shift Hypothesis for explaining *Riolama* diversification (Kok, 2013).

Downloaded from https://academic.oup.com/zoolinnean/article/190/1/271/5716277 by guest on 25 April 2024

Divergence times of Gymnophthalmoidea

Few studies so far explored diversification times within Gymnophthalmoidea (*sensu* Goicoechea *et al.*, 2016). Those who did so applied distinct fossil calibration schemes and tree-dating algorithms when compared to our approach. For instance, these studies focused on dating the Squamata tree of life, and the calibration points used were, therefore, more widely distributed within Squamata than our scheme. These previous studies used between 11 and 14 partially overlapping calibration points (Wiens *et al.*, 2006; Mulcahy *et al.*, 2012; Zheng & Wiens, 2016), with only two within Lacertoidea (*sensu* Zheng & Wiens, 2016), but distinct from the fossils used here. Also, because of the large datasets of these studies, the dating algorithms used favoured computational performance. This is the case of the Penalized Likelihood in r8s (r8s-PL) (Wiens *et al.*, 2006; Mulcahy *et al.*, 2012; Pyron & Burbrink, 2014; Zheng & Wiens, 2016), which has a better computational performance than the uncorrelated lognormal relaxed clock in BEAST (BEAST-ucld) used here. Lastly, the number of Gymnophthalmidae terminals used in different studies varied widely: Mulcahy *et al.* (2012) used three, Wiens *et al.* (2006) used 39, Pyron & Burbrink (2014) and Zheng & Wiens (2016) used 82, and our study used 63 Gymnophthalmidae terminals. In spite of these large methodological differences, the estimated timing of diversification events within Gymnophthalmidae is surprisingly similar among former studies and our analysis (Table 3). Dating algorithm, rather than calibration strategy, seems to have had an effect on estimates. The age of correspondent nodes estimated with r8s-PL was, on average, 15–17 Myr older than our estimates (Table 3), and the only estimation made with BEAST-ucld in the above studies cited (Mulcahy *et al.*, 2012) resulted in virtually the same dates as in our analysis (with the exception of Gymnophthalmidae; see Table 3), regardless of distinct molecular datasets and calibration points.

The age estimates inferred here and in previous studies (Table 3) placed the MRCA of Gymnophthalmoidea and Gymnophthalmidae in the Late Cretaceous, slightly earlier than the K/T extinction and after the breakup of the South American plate from Gondwana. This result agrees with a South American origin and restricted distribution of Gymnophthalmidae, with further dispersal of lineages into Central America. Noteworthy, there is a lack of agreement between our study and previous ones regarding the age of the MRCA of Gymnophthalminae, one of the most species-rich clades of Gymnophthalmidae. Our study places Gymnophthalminae MRCA in the Late Eocene, in contrast with an Early Eocene age estimated by studies shown in Table 3. Future studies of this topic will benefit from larger sampling of genetic and taxonomic variation in Gymnophthalmidae.

ACKNOWLEDGEMENTS

We thank Generals Sinclayer Mayer, Geraldo Miotto, Omar Zendin and Eduardo Villas Boas, Colonel Alexsandro Henriques, Lieutenant Jorge Leandro, Lieutenant Ronaldo Jose Piedade and all personnel of the Brazilian Army involved in planning and providing financial and logistical support during the Brazilian expedition to Pico da Neblina. We also thank Paulo Muzy from the University of São Paulo and the Yanomami community at Maturacá for their invaluable help during the expedition in Brazil. RWM acknowledges the field companionship in Venezuela and intellectual support provided by Alfredo Paolillo during the early stages of this project. We thank David Kizirian and David Dickey for information about Venezuelan specimens deposited at the American Museum of Natural History. Fundação de Amparo à Pesquisa do Estado de São Paulo (FAPESP 2011/50146-6, 2012/15754-8 2017/08357-6, National Science Foundation [Dimensions of Biodiversity Program (NSF (DOB 1343578), FAPESP (BIOTA 2013/50297-0), and NASA)], Coordenação de Aperfeiçoamento de Pessoal de Nível Superior [Capes]) and Conselho Nacional de Desenvolvimento Científico e Tecnológico (CNPq) provided financial support (Proc. 301778/2015-9 to MTR, 313622/2018 to PMSN). Members of the Board of Directors of the Fundacíon para el Desarrollo de las Ciencias Físicas, Matemáticas y Naturales planned and organized the expedition led by Charles Brewer-Carías in Venezuela. Support for fieldwork at Cerro Neblina was provided by Brewer-Carías and the Fundacíon and to RWM by two National Science Foundation grants (BSR 8317561 and 8317687) and a Smithsonian Institution Scholarly Studies Grant. IP acknowledges additional funding from a Smithsonian Peter Buck Postdoctoral Fellowship.

REFERENCES

Boulenger GA. 1900. Reptiles and Batrachians. In: Lankester ER. Report on a collection made by Messrs. F. V. McConnell and J. J. Quelch at Mount Roraima in British Guiana. *Transaction of the Linnean Society of London* **2:** 53–56.

Brizuela S, **Albino AM. 2016.** First Tupinambinae teiid (Squamata, Teiidae) from the Palaeogene of South America. *Historical Biology* **28:** 571–581.

Camacho A, **Rusch T**, **Ray G**, **Telemeco RS**, **Rodrigues MT**, **Angilletta MJ. 2018.** Measuring behavioral thermal

Downloaded from https://academic.oup.com/zoolinnean/article/190/1/271/5716277 by guest on 25 April 2024

tolerance to address hot topics in ecology, evolution, and conservation. *Journal of Thermal Biology* **73:** 71–79.

Castoe TA, **Doan TM**, **Parkinson CL. 2004.** Data partitions and complex models in Bayesian analysis: the phylogeny of gymnophthalmid lizards. *Systematic Biology* **53:** 448–469.

Castresana J. 2000. Selection of conserved blocks from multiple alignments for their use in phylogenetic analysis. *Molecular Biology and Evolution* **17:** 540–552.

Donadio OE. 1985. Un nuevo Lacertílio (Squamata, Sauria, Teiidae) de la Formación Lumbrera (Eoceno temprano), Província de Salta, Argentina. *Ameghiniana* **22:** 221–228.

Dowling HG, **Savage JM. 1960.** A guide to the snake hemipenis: a survey of basic structure and systematic characteristics. *Zoologica* **45:** 17–28.

Doyle AC. 1912. *The lost world*. London: Hodder & Stoughton.

Drummond AJ, **Ho SY**, **Phillips MJ**, **Rambaut A. 2006.** Relaxed phylogenetics and dating with confidence. *PLoS Biology* **4:** e88.

Emerson BC, **Gillespie RG. 2008.** Phylogenetic analysis of community assembly and structure over space and time. *Trends in Ecology & Evolution* **23:** 619–630.

Esqueda LF, **La Marca E**, **Praderio MJ. 2004.** Una nueva especie de lagarto altotepuyano del género *Riolama* (Squamata: Gymnophthalmidae) del Cerro Marahuaca, Estado Amazonas, Venezuela. *Herpetotropicos* **1:** 11–17.

Fetzner JW Jr. **1999.** Extracting high-quality DNA from shed reptile skins: a simplified method. *BioTechniques* **26:** 1052–1054.

Fick SE, **Hijmans RJ. 2017.** WorldClim 2: new 1-km spatial resolution climate surfaces for global land areas. *International Journal of Climatology* **37:** 4302–4315.

Gernhard T. 2008. The conditioned reconstructed process. *Journal of Theoretical Biology* **253:** 769–778.

Goicoechea N, **Frost DR**, **De la Riva I**, **Pellegrino KC**, **Sites Jr J**, **Rodrigues MT**, **Padial JM. 2016.** Molecular systematics of teioid lizards (Teioidea/Gymnophthalmoidea: Squamata) based on the analysis of 48 loci under tree-alignment and similarity-alignment. *Cladistics* **32:** 624–671.

Guindon S, **Dufayard JF**, **Lefort V**, **Anisimova M**, **Hordijk W**, **Gascuel O. 2010.** New algorithms and methods to estimate maximum-likelihood phylogenies: assessing the performance of PhyML 3.0. *Systematic Biology* **59:** 307–321.

Harvey MB, **Embert D. 2008.** Review of Bolivian *Dipsas* (Serpentes: Colubridae), with comments on other South American species. *Herpetological Monographs* **22:** 54–105.

Heinicke MP, **Duellman WE**, **Trueb L**, **Means DB**, **MacCulloch RD**, **Hedges SB. 2009.** A new frog family (Anura: Terrarana) from South America and an expanded direct-developing clade revealed by molecular phylogeny. *Zootaxa* **2211:** 1–35.

Hoogmoed MS. 1979. The herpetofauna of the Guianan region. In: Duellman WE, ed. *The South American herpetofauna: its origin, evolution and dispersal*. Monographs of the Museum of Natural History, the University of Kansas **7:** 241–279.

Huber O. 1987. Vegetacion y flora de Pantepui, region Guayana. *Acta Botanica Brasilica* **1:** 41–52.

Huber O. 1995. Geographical and physical features. In: Berry PE, Holst BK, Yatskievych K, eds. *Flora of Venezuelan Guayana, Vol. 1. Introduction.* St. Louis: Missouri Botanical Garden, 1–61.

Huey RB, **Deutsch CA**, **Tewksbury JJ**, **Vitt LJ**, **Hertz PE**, **Álvarez Pérez HJ**, **Garland Jr T. 2009.** Why tropical forest lizards are vulnerable to climate warming. *Proceedings of the Royal Society B: Biological Sciences* **276:** 1939–1948.

Katoh K, **Standley DM. 2013.** MAFFT multiple sequence alignment software version 7: improvements in performance and usability. *Molecular Biology and Evolution* **30:** 772–780.

Kearse M, **Moir R**, **Wilson A**, **Stones-Havas S**, **Cheung M**, **Sturrock S**, **Buxton S**, **Cooper A**, **Markowitz S**, **Duran C**, **Thierer T**, **Ashton B**, **Mentjies P**, **Drummond A. 2012.** Geneious Basic: an integrated and extendable desktop software platform for the organization and analysis of sequence data. *Bioinformatics* **28:** 1647–1649.

Kok PJR. 2009. Lizard in the clouds: a new highland genus and species of Gymnophthalmidae (Reptilia: Squamata) from Maringma tepui, western Guyana. *Zootaxa* **1992:** 53–67.

Kok PJR. 2013. *Islands in the sky: species diversity, evolutionary history, and patterns of endemism of the Pantepui Herpetofauna*. Unpublished PhD Thesis, Leiden University.

Kok PJR. 2015. A new species of the Pantepui endemic genus *Riolama* (Squamata: Gymnophthalmidae) from the summit of Murisipán-tepui, with the erection of a new gymnophthalmid subfamily. *Zoological Journal of the Linnean Society* **174:** 500–518.

Kok PJR, **MacCulloch RD**, **Means DB**, **Roelants K**, **Van Bocxlaer IV**, **Bossuyt F. 2012.** Low genetic diversity in tepui summit vertebrates. *Current Biology* **22:** 589–590.

Kok PJR, **Russo VG**, **Ratz S**, **Means DB**, **MacCulloch RD**, **Lathrop A.**, **Aubret F**, **Bossuyt F. 2016** Evolution in the South American 'Lost World': insights from multilocus phylogeography of stefanias (Anura, Hemiphractidae, *Stefania*). *Journal of Biogeography* **44:** 170–181.

Kok PJR, **Ratz S**, **MacCulloch RD**, **Lathrop A**, **Dezfoulian R**, **Aubret F**, **Means DB. 2017.** Historical biogeography of the palaeoendemic toad genus *Oreophrynella* (Amphibia: Bufonidae) sheds a new light on the origin of the Pantepui endemic terrestrial biota. *Journal of Biogeography* **45:** 26–36.

Kumar S, **Stecher G**, **Tamura K. 2016.** MEGA7: molecular evolutionary genetics analysis version 7.0 for bigger datasets. *Molecular Biology and Evolution* **33:** 1870–1874.

Lanfear R, **Frandsen PB**, **Wright AM**, **Senfeld T**, **Calcott B. 2016.** PartitionFinder 2: new methods for selecting partitioned models of evolution for molecular and morphological phylogenetic analyses. *Molecular Biology and Evolution* **34:** 772–773.

Longrich NR, **Vinther J**, **Pyron RA**, **Pisani D**, **Gauthier JA. 2015.** Biogeography of worm lizards (Amphisbaenia) driven by end-Cretaceous mass extinction. *Proceedings of the Royal Society B: Biological Sciences* **282:** 20143034.

Manzani PR, **Abe AS. 1988.** Sobre dois novos métodos de preparo do hemipênis de serpentes. *Memórias do Instituto Butantan* **50:** 15–20.

Downloaded from https://academic.oup.com/zoolinnean/article/190/1/271/5716277 by guest on 25 April 2024

Mayr E, **Phelps WH. 1967.** The origin of the bird fauna of the south Venezuelan highlands. *Bulletin of the American Museum of Natural History* **136:** 269–328.

McDiarmid RW, **Donnelly MA. 2005.** The herpetofauna of the Guayana Highlands: amphibians and reptiles of the Lost World. In: Donnelly MA, Crother BI, Guyer C, Wake MH, White ME, eds. *Ecology and evolution in the tropics: a herpetological perspective.* Chicago: University of Chicago Press, 461–560.

McDiarmid RW, **Cocroft RB**, **Paolillo A. 1988.** Preliminary field report. Herpetology collections – Cerro de la Neblina. In: Brewer-Carias C, ed. *Cerro de la Neblina. Resultados de la Expedition 1983–1987.* Caracas: Fundación para el Desarrollo de las Ciencias Físicas Matemáticas y Naturales, 665–670.

McGuire G, **Wright F. 2000.** TOPAL 2.0: improved detection of mosaic sequences within multiple alignments. *Bioinformatics* **16:** 130–134.

Milne I, **Lindner D**, **Bayer M**, **Husmeier D**, **McGuire G**, **Marshall DF**, **Wright F. 2009.** TOPALi v2: a rich graphical interface for evolutionary analyses of multiple alignments on HPC clusters and multi-core desktops. *Bioinformatics* **25:** 126–127.

Molina C, **Señaris JC. 2003.** Una nueva especie del género *Riolama* (Reptilia: Gymnophthalmidae) de las tierras altas del Estado Amazonas, Venezuela. *Memoria de la Fundacion la Salle de Ciencias Naturales* **61:** 5–19.

Mulcahy DG, **Noonan BP**, **Moss T**, **Townsend TM**, **Reeder TW**, **Sites Jr JW**, **Wiens JJ. 2012.** Estimating divergence dates and evaluating dating methods using phylogenomic and mitochondrial data in squamate reptiles. *Molecular Phylogenetics and Evolution* **65:** 974–991.

Müller J, **Hipsley CA**, **Head JJ**, **Kardjilov N**, **Hilger A**, **Wuttke M**, **Reisz RR. 2011.** Eocene lizard from Germany reveals amphisbaenian origins. *Nature* **473:** 364.

Myers CW, **Donnelly MA. 2001.** Herpetofauna of the Yutaje-Corocoro massif, Venezuela: second report from the Robert G. Goelet American Museum-Terramar expedition to the northwestern tepui. *Bulletin of the American Museum of Natural History* **261:** 1–85.

Myers CW, **Rivas Fuenmayor G**, **Jadin RC. 2009.** New species of lizards from Auyantepui and La Escalera in the Venezuelan Guayana, with notes on 'microteiid' hemipenes (Squamata: Gymnophthalmidae). *American Museum Novitates* **3660:** 1–31.

Nunes PMS. 2011. *Morfologia hemipeniana dos lagartos microteídeos e suas implicações nas relações filogenéticas da família Gymnophthalmidae (Teiioidea: Squamata).* Unpublished DPhil. Thesis, Universidade de São Paulo.

Nunes PMS, **Fouquet A**, **Curcio FF**, **Kok PJR**, **Rodrigues MT. 2012.** Cryptic species in *Iphisa elegans* Gray, 1851 (Squamata: Gymnophthalmidae) revealed by hemipenial morphology and molecular data. *Zoological Journal of the Linnean Society* **166:** 361–376.

Pellegrino KC, **Rodrigues MT**, **Yonenaga-Yassuda Y**, **Sites Jr JW. 2001.** A molecular perspective on the evolution of microteiid lizards (Squamata, Gymnophthalmidae), and a new classification for the family. *Biological Journal of the Linnean Society* **74:** 315–338.

Pesantes OS. 1994. A method for preparing the hemipenis of preserved snakes. *Journal of Herpetology* **28:** 93–95.

Pyron RA, **Burbrink FT. 2014.** Early origin of viviparity and multiple reversions to oviparity in squamate reptiles. *Ecology Letters* **17:** 13–21.

R Core Team. **2019.** *R: a language and environment for statistical computing*. Vienna: R Foundation for Statistical Computing, www.R-project.org/.

Rambaut A, **Drummond AJ**, **Xie D**, **Baele G**, **Suchard MA. 2018.** Posterior summarisation in Bayesian phylogenetics using Tracer 1.7. *Systematic Biology* **67:** 901–904.

Recoder RS, **Magalhães Jr A**, **Rodrigues J**, **Pinto HBA**, **Rodrigues MT**, **Camacho A. 2018.** Thermal constraints explain the distribution of the climate relict lizard *Colobosauroides carvalhoi* (Gymnophthalmidae) in the semiarid caatinga. *South American Journal of Herpetology* **13:** 248–260.

Ronquist F, **Teslenko M**, **Van der Mark P**, **Ayres DL**, **Darling A**, **Höhna S**, **Larget B**, **Liu L**, **Suchard MA**, **Huelsenbeck JP. 2012.** MrBayes 3.2: efficient Bayesian phylogenetic inference and model choice across a large model space. *Systematic Biology* **61:** 539–542.

Rull V. 2004. Biogeography of the 'Lost World': a palaeoecological perspective. *Earth-Science Reviews* **67:** 125–137.

Salerno PE, **Ron SR**, **Señaris JC**, **Rojas-Runjaic FJ**, **Noonan BP**, **Cannatella DC. 2012.** Ancient tepui summits harbor young rather than old lineages of endemic frogs. *Evolution* **66:** 3000–3013.

Savage JM. 1997. On terminology for the description of the hemipenis of squamate reptiles. *Herpetological Journal* **7:** 23–25.

Steyermark JA. 1986. Speciation and endemism in the Flora of the Venezuelan tepuis. In: Vuilleumier F, Monasterios M, eds. *High altitude tropical biogeography.* New York: Oxford University Press, 317–373.

Steyermark JA, **Berry PE**, **Holst BK**, **Yatskievych K. 1995.** *Flora of the Venezuelan Guayana. Vol. 1.* St. Louis: Missouri Botanical Garden.

Strangas ML, **Navas CA**, **Rodrigues MT**, **Carnaval AC. 2019.** Thermophysiology, microclimates, and species distributions of lizards in the mountains of the Brazilian Atlantic forest. *Ecography* **42:** 354–364.

Suchard MA, **Lemey P**, **Baele G**, **Ayres DL**, **Drummond AJ**, **Rambaut A. 2018.** Bayesian phylogenetic and phylodynamic data integration using BEAST 1.10. *Virus Evolution* **4:** vey016.

Sullivan RM, **Estes R. 1997.** A reassessment of the fossil Tupinambinae. In: Kay RF, Madden RH, Cifelli RL, Flynn JJ, eds. *Vertebrate paleontology in the Neotropics, the Miocene fauna of La Venta, Colombia*. Washington, DC: Smithsonian Institution Press, 100–112.

Sullivan J, **Joyce P. 2005.** Model selection in phylogenetics. *Annual Review of Ecology, Evolution, and Systematics* **36:** 445–466.

Uzzell T. 1973. A revision of the genus *Prionodactylus* with a new genus for *P. leucostictus* and notes on the genus *Euspondylus* (Sauria, Teiidae). *Postilla* **159:** 1–67.

Downloaded from https://academic.oup.com/zoolinnean/article/190/1/271/5716277 by guest on 25 April 2024

Vaidya G, **Lohman DJ**, **Meier R. 2011.** SequenceMatrix: concatenation software for the fast assembly of multi-gene datasets with character set and codon information. *Cladistics* **27:** 171–180.

Wiens JJ, **Brandley MC**, **Reeder TW. 2006.** Why does a trait evolve multiple times within a clade? Repeated evolution of snakeline body form in squamate reptiles. *Evolution* **60:** 123–141.

Wiens JJ, **Camacho A**, **Goldberg A**, **Jezkova T**, **Kaplan ME**, **Lambert SM**, **Miller EC**, **Streicher JW**, **Walls RL. 2019.** Climate change, extinction, and sky island biogeography in a montane lizard. *Molecular Ecology* **28:** 2610–2624.

Zaher H. 1999. Hemipenial morphology of the South American xenodontine snakes, with a proposal for a monophyletic Xenodontinae and a reappraisal of colubroid hemipenes. *Bulletin of the American Museum of Natural History* **240:** 1–168.

Zheng Y, **Wiens JJ. 2016.** Combining phylogenomic and supermatrix approaches, and a time–calibrated phylogeny for squamate reptiles (lizards and snakes) based on 52 genes and 4162 species. *Molecular Phylogenetics and Evolution* **94:** 537–547.

SUPPORTING INFORMATION

Additional Supporting Information may be found in the online version of this article at the publisher's web-site.

Table S1. List of samples retrieved from Genbank and included in molecular analyses, with accession numbers. Systematic classification follows Goicoechea *et al.*, 2016.

Table S2. Comparative table highlighting variation in morphological characters among the six species of *Riolama* presently known.

Downloaded from https://academic.oup.com/zoolinnean/article/190/1/271/5716277 by guest on 25 April 2024